REFERENCES FOR SECTION 3

1. T.R. Walsh. 'Provisional Selection of Some Injector Parameters' Internal Report HAG/INJ/7

2. R. Taylor. 'Calculation of Drift-Tube Dimensions in the Linac Injector for the 7 GeV Harwell Proton Synchrotron' A.E.R.E/R3012

3. R. Taylor. 'Acceptance of Axially and Radially Oscillating Particles in the Linac Injector for Nimrod' A.E.R.E./R3013

4. R. Taylor. 'Effects of Rotational Misalignments on the Radial Acceptance of the Linac Injector for Nimrod' A.E.R.E./R3096

5. E. Regenstreif. 'The CERN Proton Synchrotron. Chapter 5 Injection' CERN Report 60-26

6. CERN Internal Report PS/3396; MPS/Int. LIN 62-3

7. J.R. Pierce. 'Theory and Design of Electron Beams' D. Van Nostrand, New York

8. L.C.W. Hobbis et al. 'Plasma Physics' Vol.1, pp 130-134.

9. J.J. Wilkins. 'Design Notes on Resonators on Proton Linear Accelerators' A.E.R.E. GP/R1613

10. N.D. West. 'R.F. Model Measurements for the Injector Linac' Internal Report HAG/INJ/11.

11. J.T. Hyman. 'Design of Quadrupole Focusing Magnets' Internal Report HAG/INJ/9.

12. J.T. Hyman. 'Quadrupole Dimensions for the Synchrotron Injector Linac'. Internal Report HAG/INJ/12.

13. J.T. Hyman. 'Modified Design and Dimensions for the Injector Linac Quadrupoles' Internal Report HAG/INJ/14

14. R. Billinge. 'Beam Steering in the Nimrod Injector System' Internal Report HAG/INJ/16

15. J.T. Hyman. 'Some High Current Circuits Using Transistors' NIRL/R/17

16. R. Billinge. 'An Achromatic Inflector System for Nimrod' AERE/R3475

17. M. Bell. 'Injection into the 7 GeV Synchrotron' AERE/T/M155

18. J.T. Hyman. 'Injector Control Room Pulse Timing System' Internal Report HAG/INJ/24.

SECTION 4

MAGNET AND ASSOCIATED SYSTEMS

The Nimrod magnet is made up of eight sections (octants) separated by nominally field-free regions (straight sections). The magnet yoke of each octant contains 42 sectors. Early design information(1) and a description of the sectors(2) are already available. Details of the foundations for the magnet ring are also published(3).

4.1. Sector Testing

It can be shown that azimuthal variations of the guide field, B_z, lead to variations in the radial position of the proton closed orbit in the machine. This is equivalent to a loss of radial aperture; e.g. a first harmonic variation of B_z with amplitude $\frac{\Delta B_z}{B_z} = \frac{4}{10^4}$ leads to a loss of radial aperture of 1 inch.

Each magnet sector was therefore compared with a reference sector on receipt from the manufacturers to determine the following characteristics:-

(i) Value of remanent field

(ii) Relative values of field produced by current in the energising coils at values of field in the gap varying from 200 to 14,000 gauss

(iii) Eddy current effects.

The electronic measuring equipment(4), the model (see Fig. 4.1(i)) and its power supply have been described elsewhere(5). The measurement programme took about sixteen months.

4.1.1. Results of Tests

Variations in the value of the remanent field and hence the value of gap field at low pulsed fields were the most noticeable. Fig. 4.1(ii) shows the value of the remanent field plotted against the order in which the sectors were manufactured. It is very noticeable that early sectors had a very much higher remanent field (up to 24 gauss) than later sectors. This was due to the fact that it was not possible to manufacture the whole quantity of steel in one batch and randomise completely. The steel which had been annealed early in the programme was the cause of the high remanence and was present in sectors up to about number 245.

The largest variation in relative field at low fields was directly due to variations in remanent field values. This is shown on Fig. 4.1(iii) which has a band containing the result of plotting relative fields at 200 gauss against remanent field. The width of the band was about 1.3%, or 2.6 gauss, compared with a remanent field band of 12 gauss. This graph also shows the interdependance of remanent field and low field permeability; viz, sectors with high remanent field have low permeability and hence relatively low pulsed field values at low fields.

There were differences in remanent fields measured for a given sector with the high and low dB/dt at low fields. In general the remanent fields of all sectors were lower with the higher dB/dt, and sectors with low remanent fields were depressed more at the higher dB/dt.

An attempt to measure eddy current effects was made using a saturating choke to vary dB/dt at 200 gauss. No variations in relative field outside the measurement accuracy were found for the two rates of rise.

The relative variation of gap field at 10 kilogauss is shown in Fig. 4.1(iv) and that for 14 kilogauss in Fig. 4.1(v). There was only slight correlation between gap field and sector weight (i.e. magnet cross-section or flux density) at 14 kilogauss. Polepieces on the test model with larger radial extent would have been an advantage in showing up high field permeability effects.

4.1.2. Distribution of Sectors Around Magnet

In order to prevent delay in placing sectors in correct positions on the monolith, allocation of sector positions as a result of the tests were made continuously as testing proceeded. End-of-octant sectors were chosen as those with good high field results and large weight since the end sectors were required to carry more fringe flux at high fields. Sectors were also required here with good mechanical shape i.e. constant width with radius along the gap. Eight sectors with similar properties at low fields were then allocated the same relative positions in each octant. Batches of eight sectors were then continuously allocated in such a way as to keep the total relative field in each octant and with equal distribution within a quarter of each octant. As described above the largest variation was at 300 gauss but a similar check on total field was kept at 600, 10,000 and 14,000 gauss. As an added insurance, at high fields the total weight per octant was equalised. The difference in remanent field for the different dB/dt values was also equalised.

The results of this exercise were gratifying. At 300, 10,000 and 14,000 gauss the average error per octant was adjusted to be lower than the accuracy of measurement (a few parts in 10^4). The total variation in octant weight was 12 hundredweight or about 0.1%; individual sectors varied by as much as 4 hundredweight.

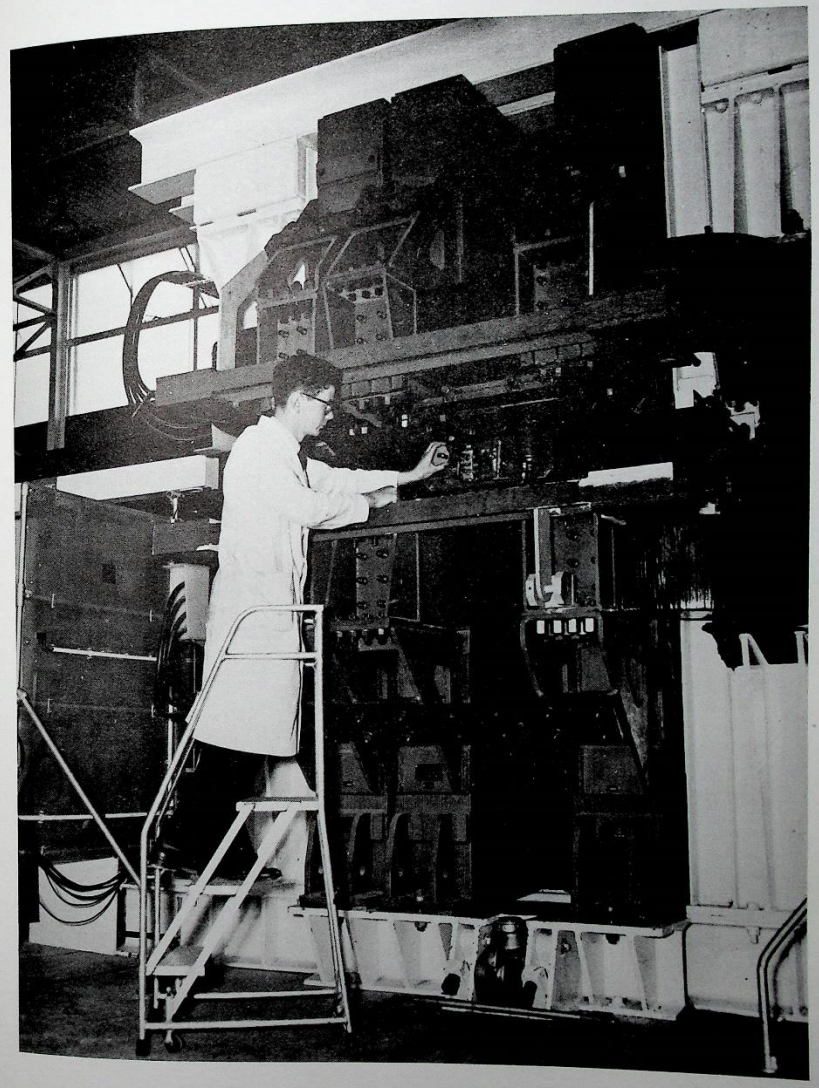

Fig. 4.1(i) Magnet model IV used for sector comparison.

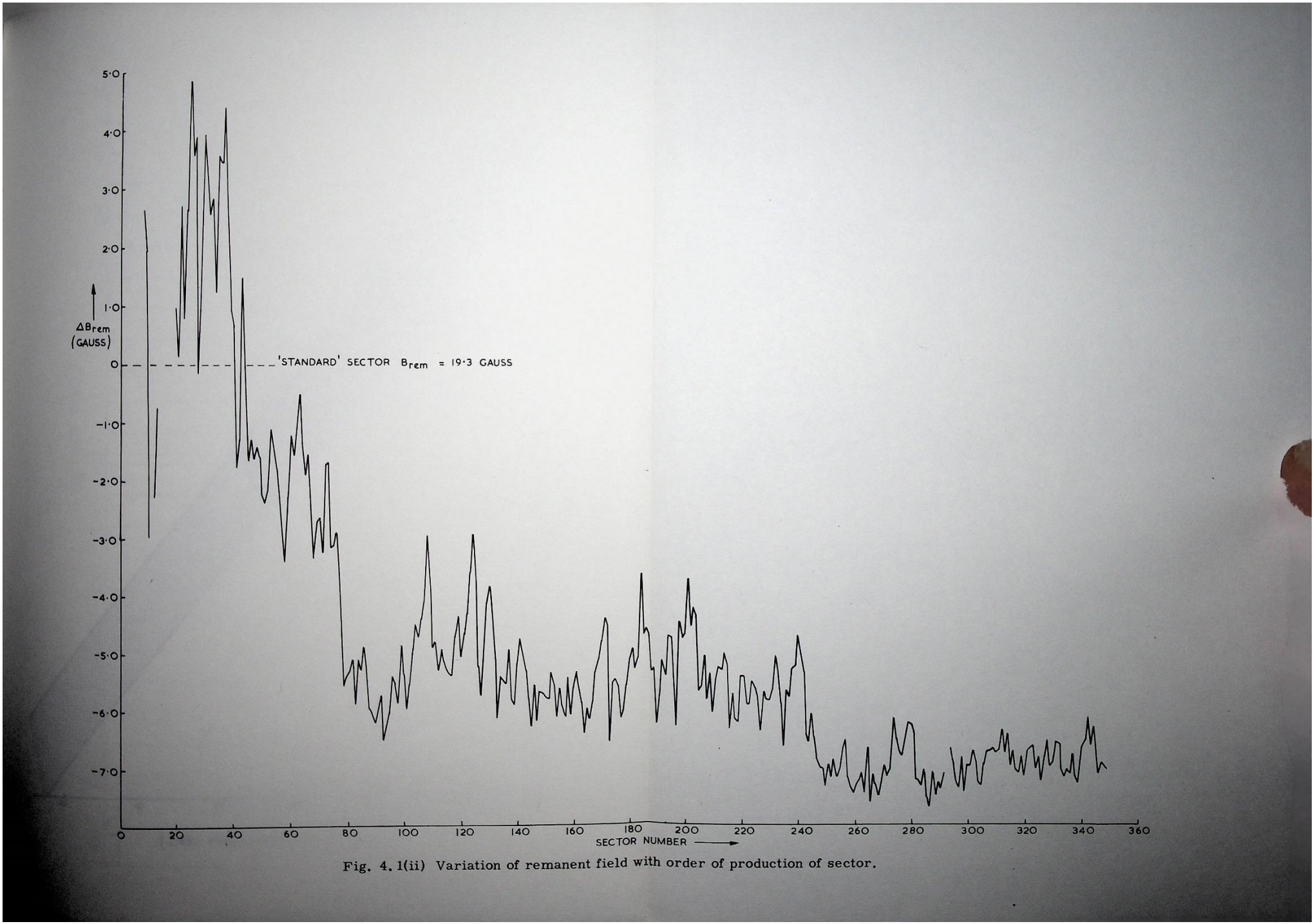

Fig. 4. 1(ii) Variation of remanent field with order of production of sector.

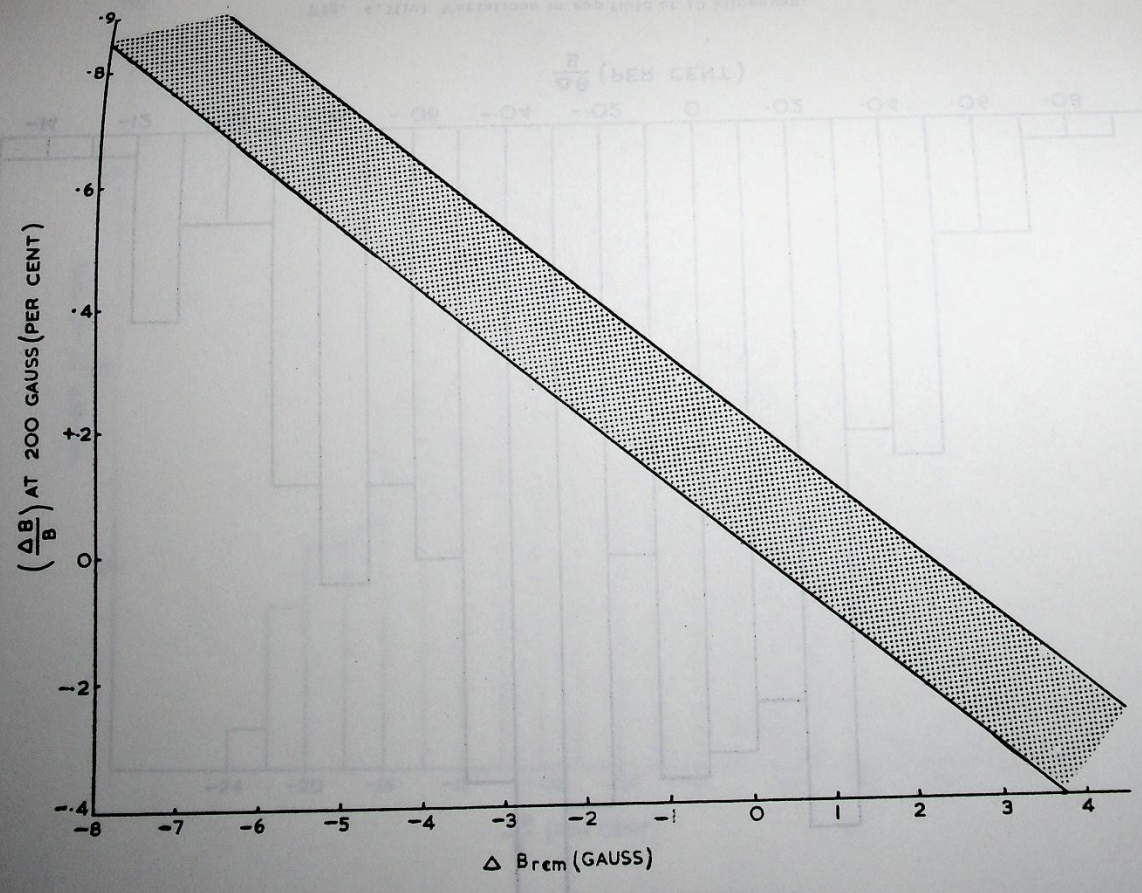

Fig. 4.1(iii) Variation of low field properties with remanent field.

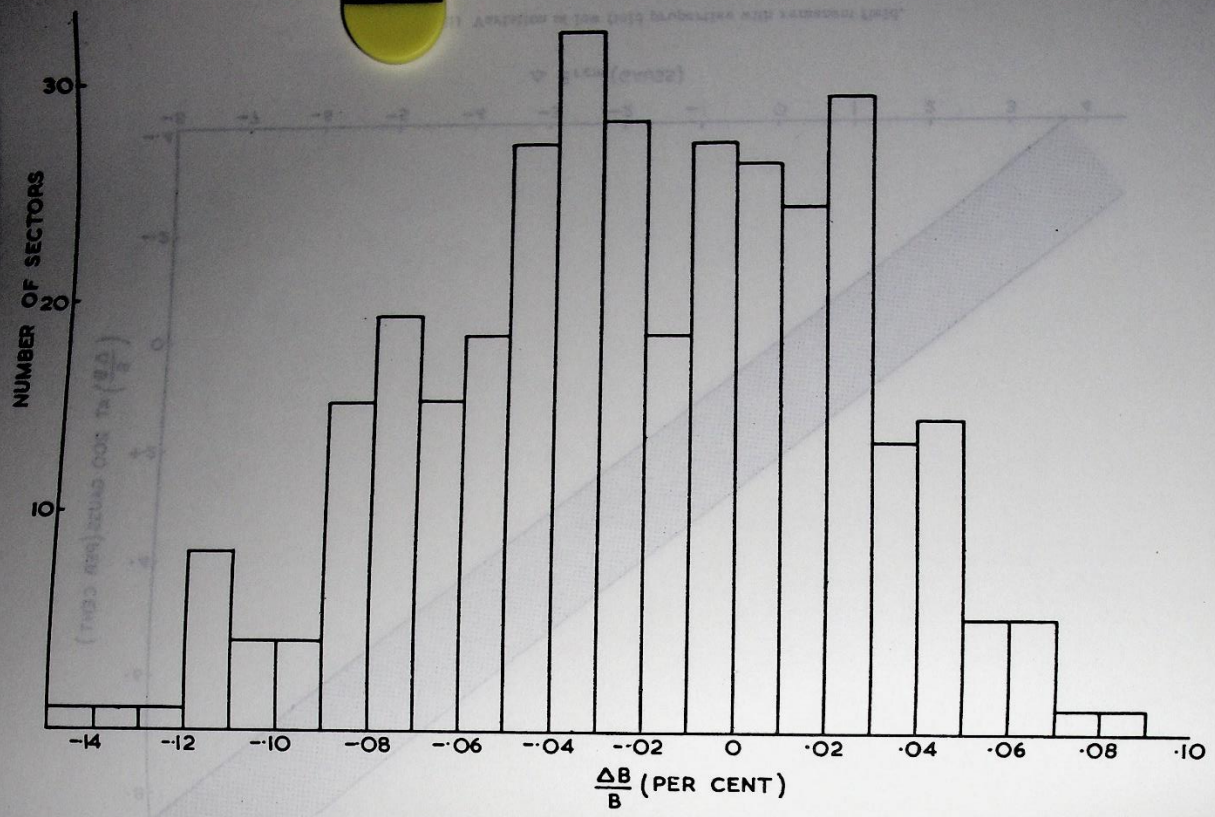

Fig. 4.1(iv) Variations in gap field at 10 kilogauss.

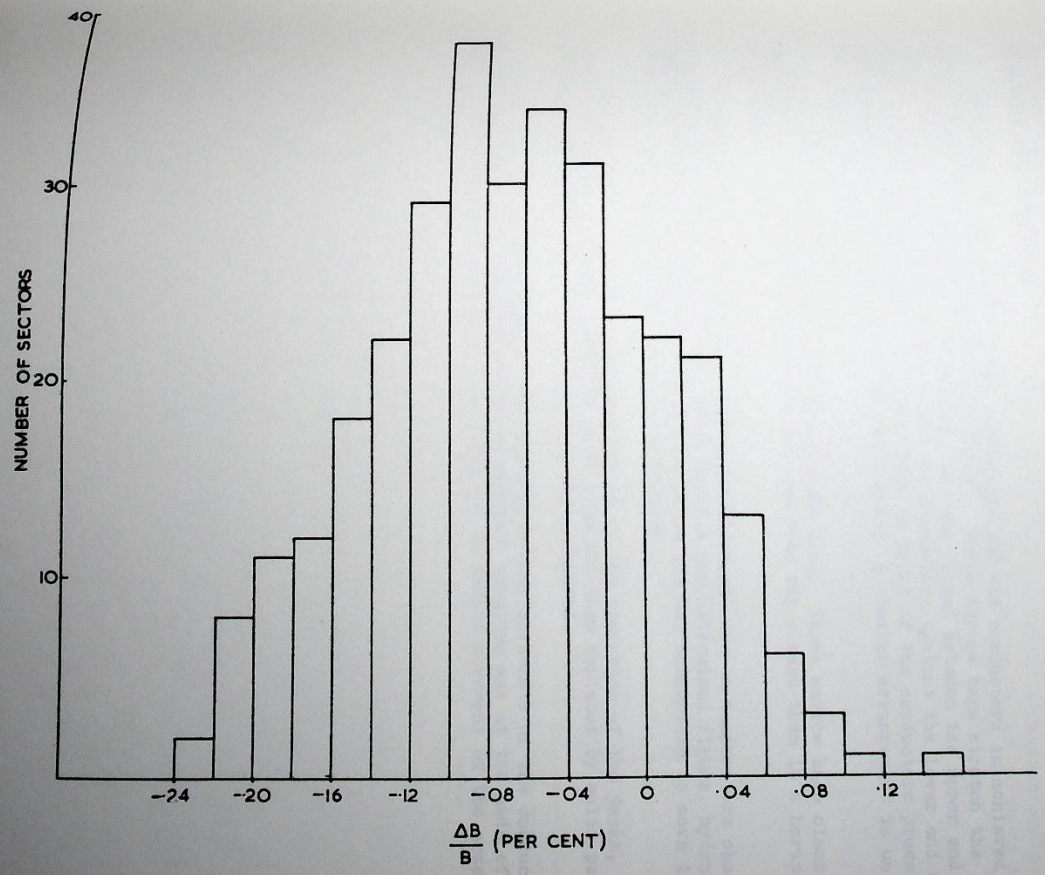

Fig. 4.1(v) Variations in gap field at 14 kilogauss.

4.2. Main Coils

During the early part of 1962 the installation of the longitudinal conductors, end conductors, and all the steel work connected with the octant and magnetic shielding was completed.

Clamping of the longitudinal conductors and end conductors is achieved by means of air bags pressurised to 25 lb/in^2. Three narrow bags stretch the length of the throat longitudinal conductors, and are placed between the upper and lower sets of conductors. These bags clamp the conductors against the lower and upper faces of the coil aperture. Two wide bags in front of the conductors press the conductors back into the throat of the magnet. A similar arrangement is used for the lip conductors.

The end conductors are held by air bags also. Three narrow bags clamp the conductors in a vertical direction, and one wide bag clamps them in a horizontal direction.

To allow for coil movement (and end conductors) due to temperature changes, e.g. when the coil cooling water drops below a pre-determined figure, hydraulic jacks used as stops could be operated to allow the end conductors to move inwards, after the vertical air bags had been evacuated.

A good deal of trouble was experienced in the operation of the jacks, oil leaks, sticking rams etc., and the jacks have now been replaced by solid paxolin packers, which can be released manually when required.

During the early stages of the pulsing various movements of the conductors where measured. The maximum amount of movement observed was at the ends of the upper lip conductors which at each pulse had an upward movement of the order of 18 thou.

4.3. Main Polepieces

4.3.1. Design and Measurements

The main Nimrod polepieces are designed from the basic ideas detailed in (6). Briefly, saturable 'fins' are used at the radial edges of the polepieces in order to reduce the total flux to be carried by the magnet sectors at high gap fields. A design was chosen to save about 5% total flux at peak field. The aim was to obtain 36 in of useful field at injection and 14 in at peak field by using shims at both low and high fields.

For ease of construction of the poles, the shape of the laminations as used on small-scale poles was changed somewhat. The 'inner' lamination was made with the same profile as the 'outer' lamination except for the working profile (see Fig. 4.3(i)). To attain a pole with an effective fin corresponding to an 'f' of about 0.32 (f is the ratio of the amount of steel in a fin to the amount of steel if it were solid) holes were cut in both laminations. The holes were so arranged as to arrive at an effective pole at high field which was similar to the shape of the earlier 'inner' laminations. Since the flux in the fin when saturated has a direction corresponding to about 45^{o}, matching of the saturation effects due to an f of 0.32 fin, requires an $f \sim 0.25$ in the crenellated region of the correction shims. (The n-values for an uncorrected pole are shown in Fig. 4.3(ii)). The inner lamination was .020 in thick 4% silicon steel; the outer was .030 in thick 1% silicon steel. The high field correction shims were designed with the aid of small-scale(7) (8) and full-scale (5) models. The basic method of correction is given in (6). If the height of the shim on the inner hidden lamination is d, the effective height of shim is $d(H/B_o)$, H being the field in the saturating steel and B_o the flux density in the magnet gap. Simple shim theory is used to predict the corrections. In our case a match cannot be made (above about 10 kilogauss) between the correction due to the shims and the error in n as field varies. Three types of laminations with shims of different height are therefore used; the shallow recess corrects up to about 10 kilogauss, this lamination starts to saturate forming a crenellation with a different f value ($\sim$0.32) and gives a correction due to the shim on the medium recess lamination. This gives correction up to about 13 kilogauss. This lamination in turn begins to saturate giving a third f value with correction due to the shim on the deep recessed lamination. The corrections due to the three different f values are additive. The necessary f-values are obtained by adjusting the numbers of the different types of lamination. Correction of the base line of n is required at high fields; for this reason there is a superimposed slope on the medium and deep recessed laminations as described by the Saclay group(9). A more detailed report on the design of the polepieces will be published later.

The design of the low field shims is based on (10). The field shapes at low field levels for the production poles when measured on Model V are shown in Fig. 4.3(iii). The high field shapes are given in Fig. 4.3(iv). It can be seen that the correction at the higher fields is not particularly good. This is thought to be due to differences in steel and incorrect allowance for packing factor on extrapolating from bolted up poles to bonded poles. For this reason and because of octant end effects discussed in section 4.4, Mark II poles were designed. These were made from laminations of the same profile but with different ratios of the various laminations (see Fig. 4.3(v)). The field shapes for these poles as measured on Model V are given in Fig. 4.3(vi).

0·020 IN. THICK LAMINATION
(NOTCHED)

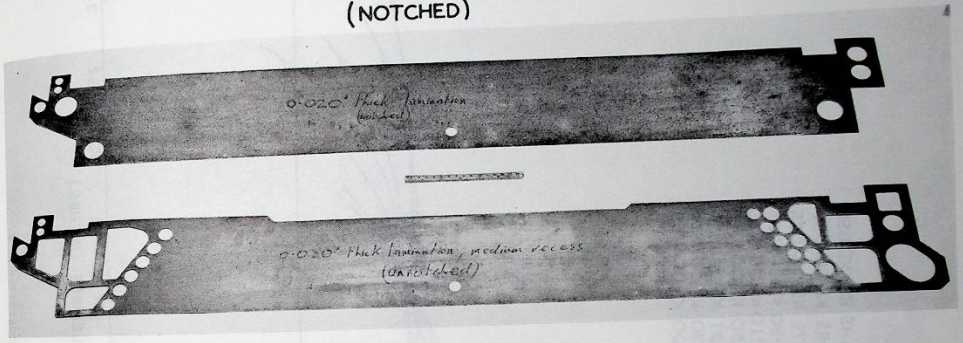

0·030 IN. THICK LAMINATION
MEDIUM RECESS (UNNOTCHED)

0·030 IN. THICK LAMINATION
DEEP RECESS (NOTCHED)

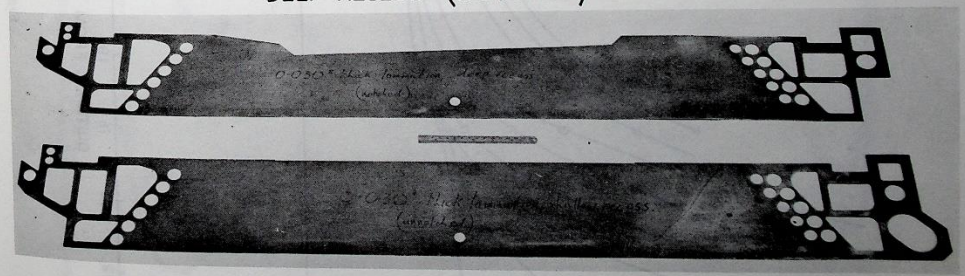

0·030 IN. THICK LAMINATION
SHALLOW RECESS (UNNOTCHED)

Fig. 4.3(i) Polepiece laminations.

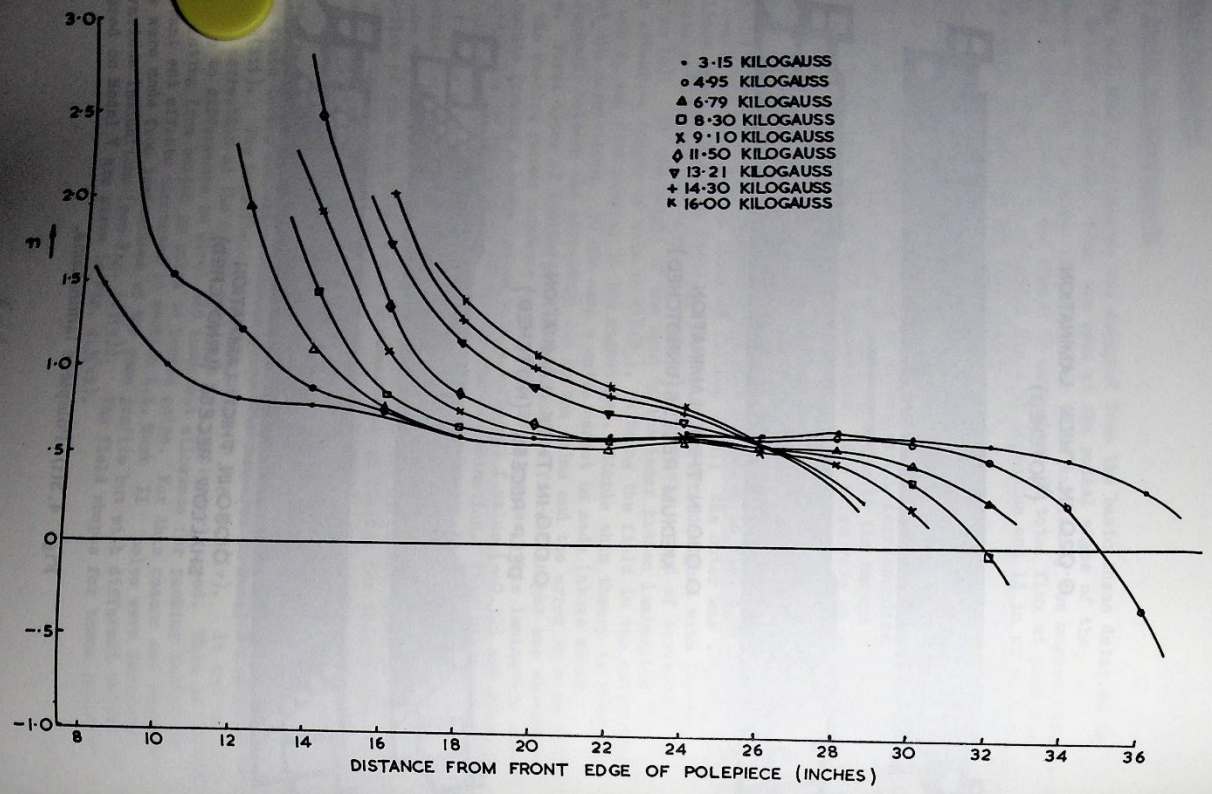

Fig. 4.3(ii) n values for uncorrected pole.

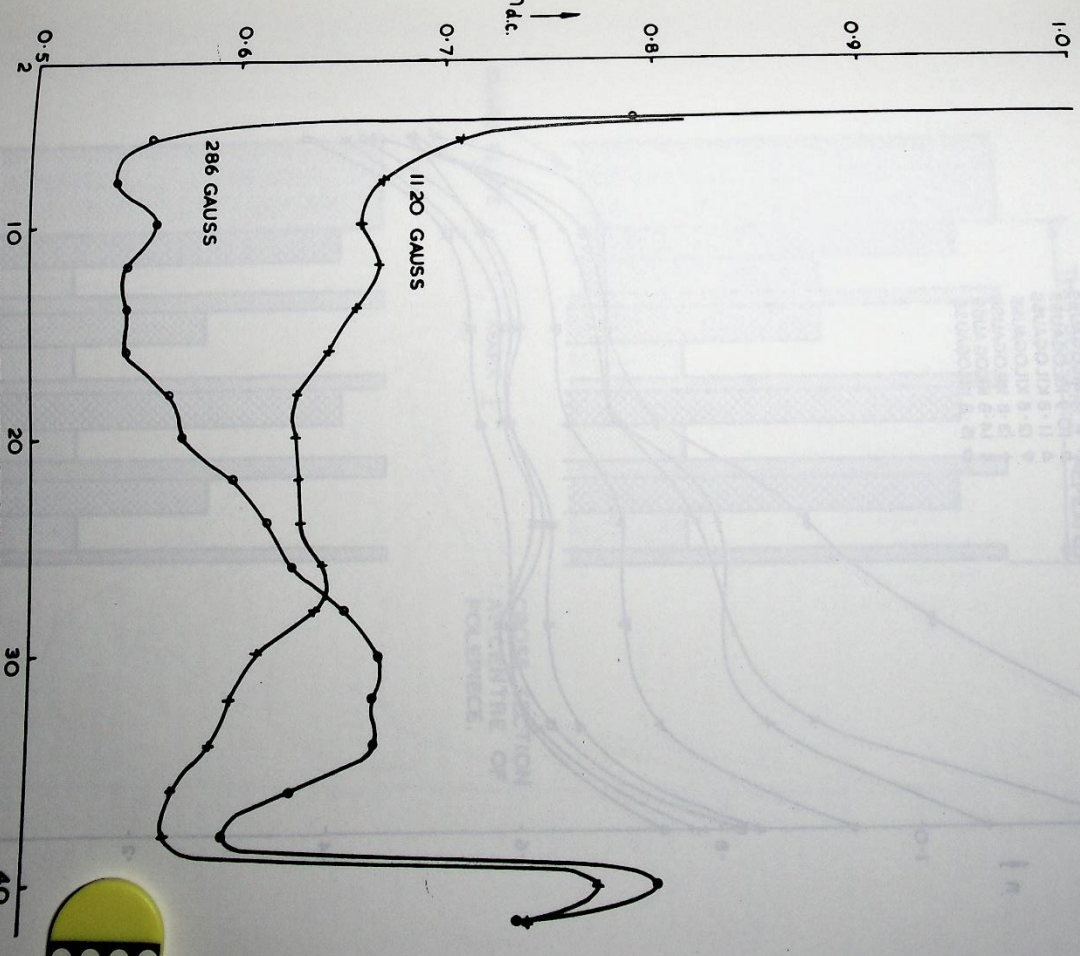

Fig. 4.3(iii) n values at low fields. Production poles on Model V.

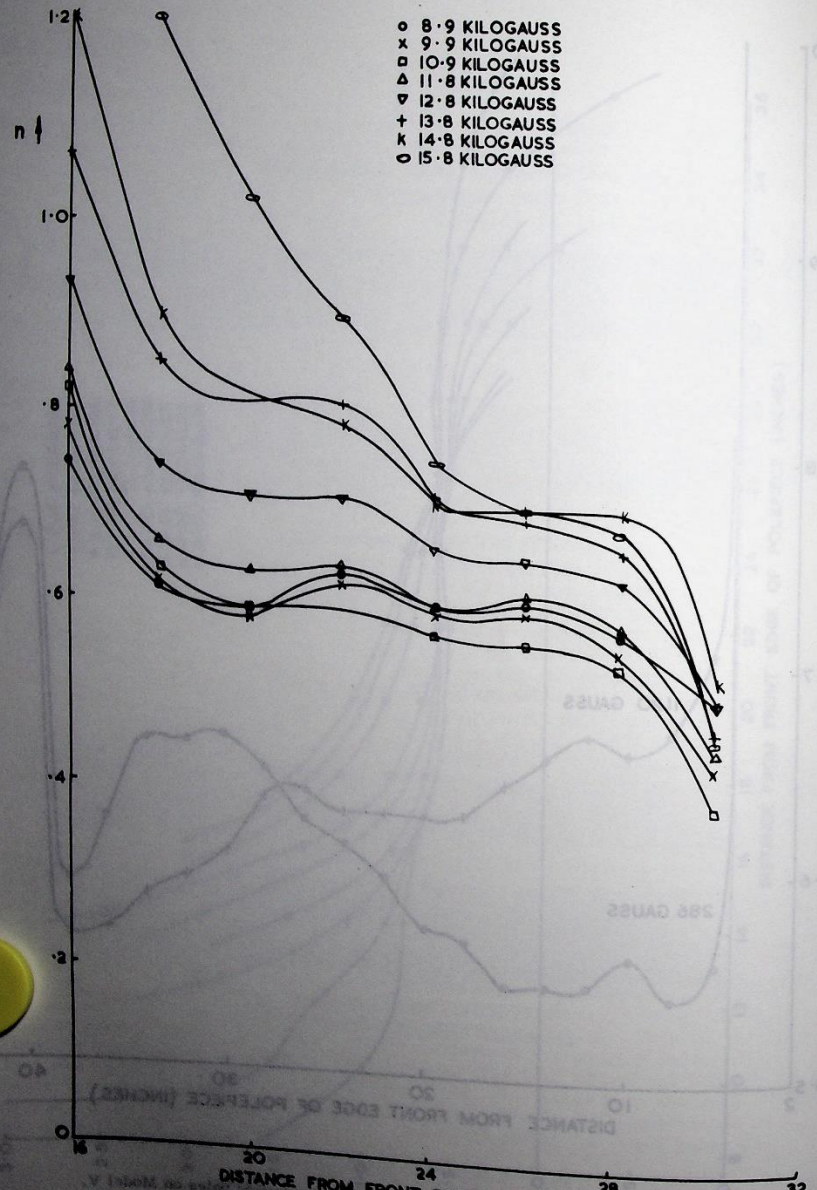

Fig. 4.3(iv) n values at high fields. Production poles on Model V.

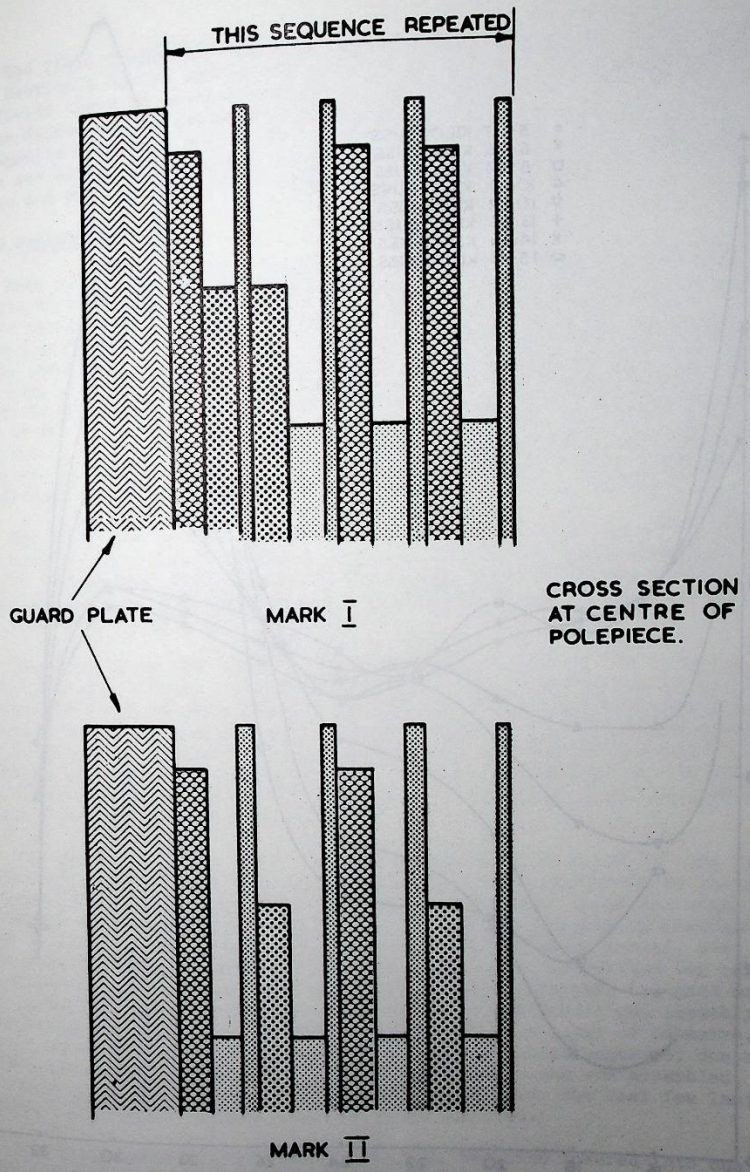

Fig. 4.3(v) Polepiece lamination arrangements.

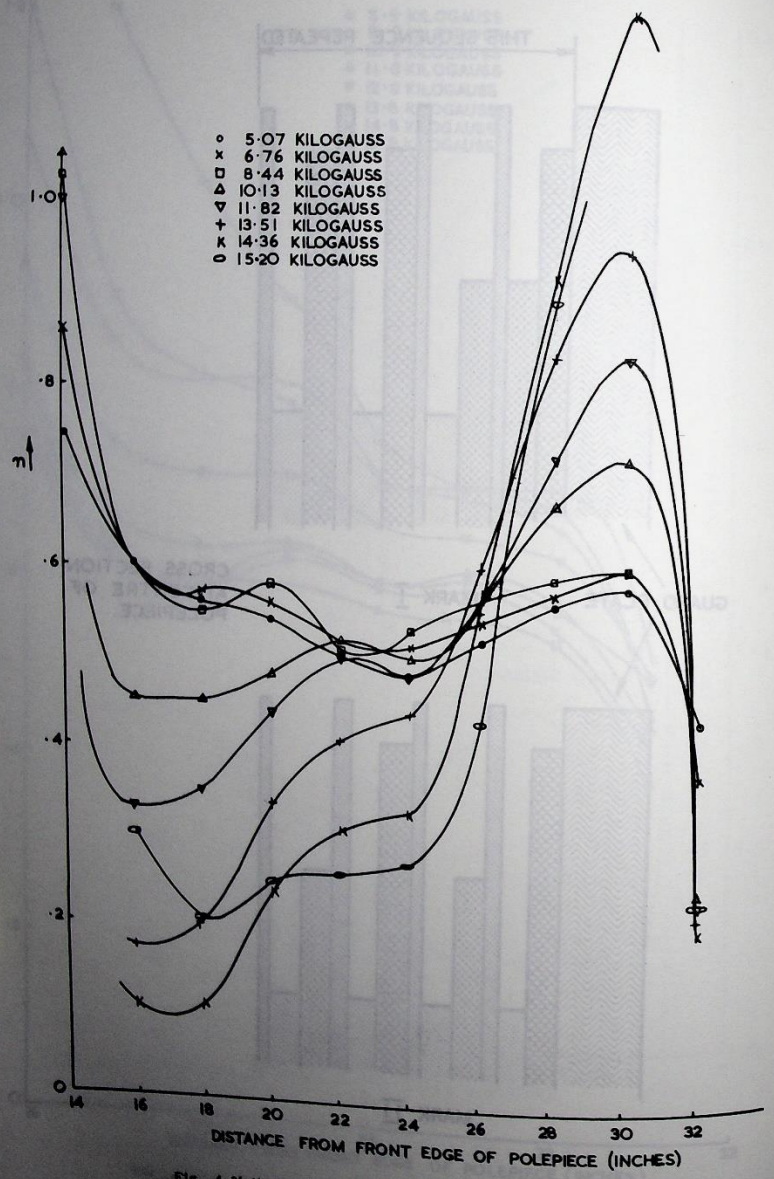

Fig. 4.3(vi) n values for Mark II polepieces on Model V.

The field shapes for the main poles measured during the Nimrod magnetic survey (see Section 4.6) are shown in Fig.4.3(vii), 4.3(viii) and 4.3(ix), these show that at low fields there is greater correction than on Model V. This is most probably due to the difference in energising coil configurations and the difference in the amount of magnetic materials around the coils in the two cases. At high fields, too, there are differences between Model V and the Nimrod magnet. These are probably due to end effects of Model V which is only 7 sectors long.

4.3.2, Manufacture

Each of the 336 magnet sectors is fitted with a pair of polepieces which are positioned between the inner and outer vacuum vessels and support the thin wall of the outer vessel against atmospheric pressure. Special polepieces are used on the end sectors of each octant to achieve the required magnetic field distribution in the straight sections. The assembled main polepiece is approximately 48 in long, 6 in deep and 13½ in wide and is built up from approximately 450 laminations (0.020 in and 0.030 in thick) with a ¼ in thick guard or reinforcing plate on each side of the stack of laminations. It weighs about 800 lb. Each lamination is insulated from its neighbours, the insulation being a 0.002 in layer of epoxy resin adhesive, bonding the whole assembly solidly together. These glued joints resist the disruptive magnetic forces.

The guard plates are of a low silicon electrical quality steel identical to that used for the magnet sectors. The thin (0.020 in) laminations are a high quality transformer steel, about 3.5% silicon, with high permeability at low flux densities, whereas the thick (0.030 in) laminations are a low silicon steel with high permeability at high flux densities.

The polepieces are assembled with alternate thick and thin laminations in the ratio; 2 thick, 1 thin, 2 thick, 1 thin, etc. It was necessary to hold all the material in stock so that complete "shuffling" could take place prior to cutting to shape, to ensure a uniformity of magnetic properties in all polepieces which were produced in "matched" pairs. In addition, the laminations had to be cut and assembled in such a way that effects of taper and "crowning" of the rolled sheets were minimised and uniformity of thickness of assembled poles from start to finish of the production run were maintained.

The quarter million or so laminations had to be produced to very fine dimensional tolerances and variation of profile from lamination to lamination did not exceed 0.004 in. The laminations have a network of holes and slots arranged to achieve the required magnetic field. The general process of manufacture was to shear to overall size, pierce the holes, deburr, degrease, anneal, sort into pairs, blank profile, deburr, inspect, degrease and prepare the surface for adhesive. For the assembly, some very massive and rigid assembly jigs were designed and poles were assembled, prior to glueing, in a special clean conditions assembly room. A guard plate was first laid in the jig followed by a layer of adhesive, a lamination, a layer of adhesive, etc., all in a carefully controlled sequence, controlling weights as assembly progressed, until the complete stack was assembled. A slight modification to the assembly sequence was allowed over the last few laminations to permit the weight tolerance of ±1% to be achieved.

The whole assembly, complete in the jig, was then lowered into one of three specially designed curing ovens and subjected to a carefully controlled pressure to ensure dimensional correctness as the adhesive became fluid when subject to the

curing heat. The heating cycle was also very carefully controlled and consisted of approximately 3½ hours to heat to 158°C, held at this temperature for 4½ hours and then allowed to cool over a further 6/7 hours.

After cooling, the assembled pole was carefully cleaned of surplus resin. A small amount of machining of a taper on the guard plates was completed on a milling machine and the pole was then subjected to an exhaustive range of insulation, dimensional and strength tests. When passed final inspection poles were packed, two pairs in a specially designed transport box, and transported to Nimrod.

The production of the poles, including the very extensive development period when manufacturing techniques were established and final profile shapes were worked out (from a very limited number of experimental poles) occupied a period of 24 months.

Liaison was necessary at all times with the manufacturers and an elaborate series of manufacturing specifications were produced to cover each stage of production in great detail.

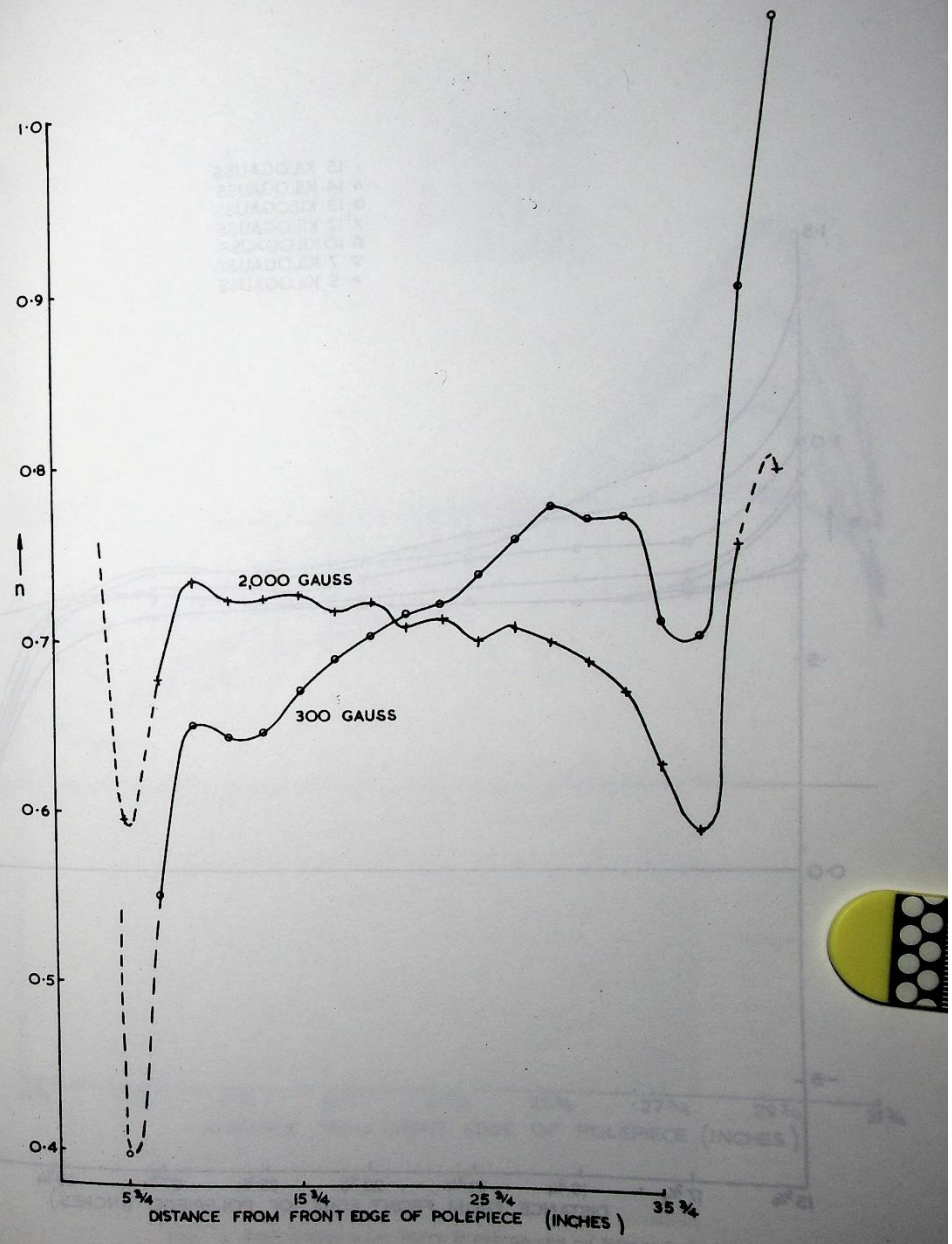

Fig. 4.3(vii) n values at low fields on Nimrod.

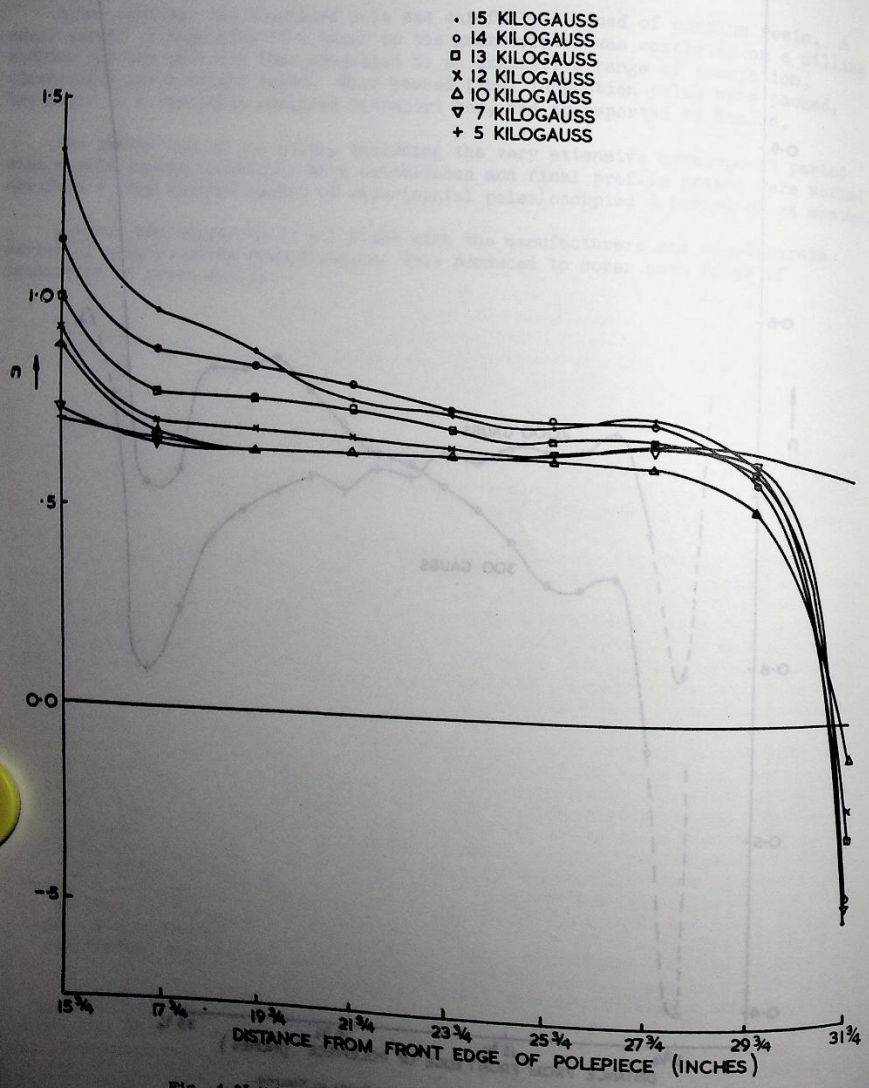

Fig. 4.3(viii) n values for Mark I polepieces on Nimrod at high fields.

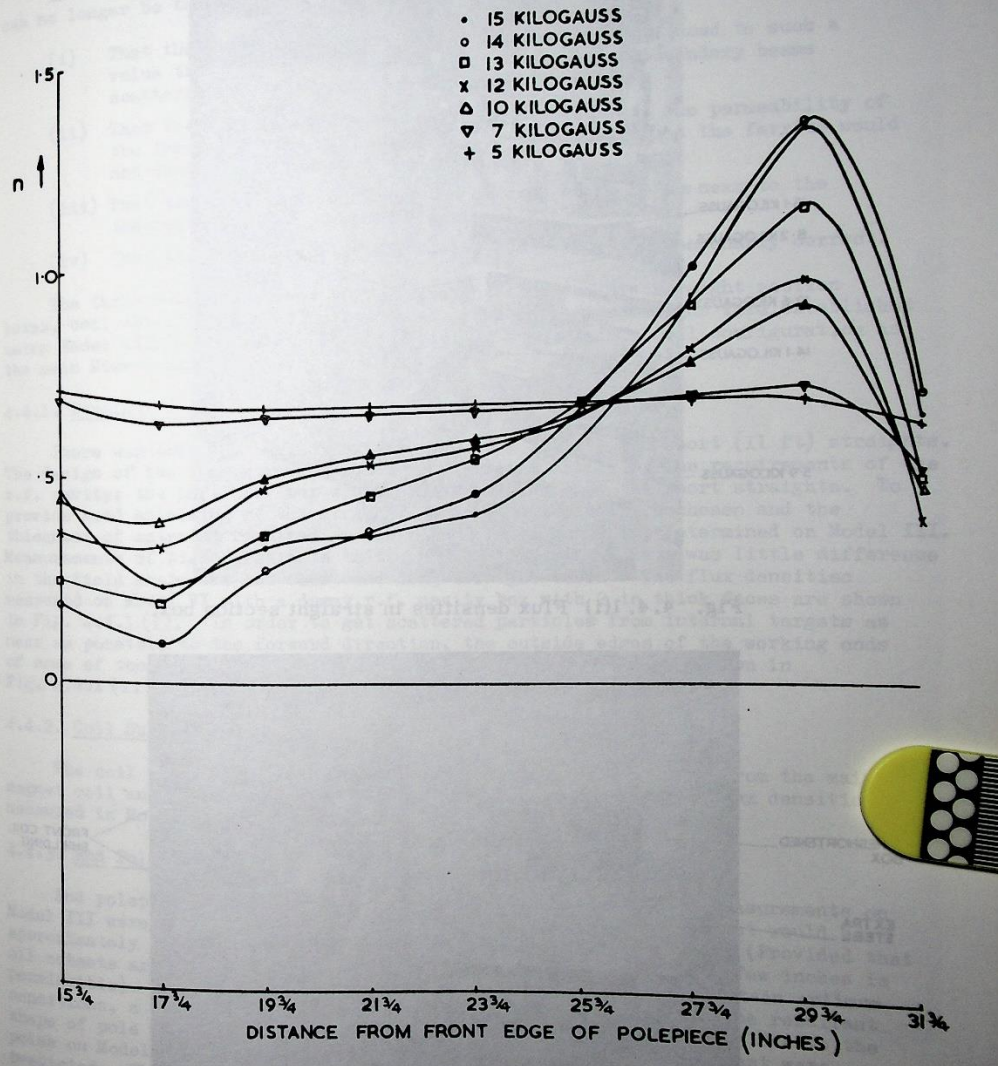

Fig. 4.3(ix) n values for Mark II polepieces on Nimrod at high fields.

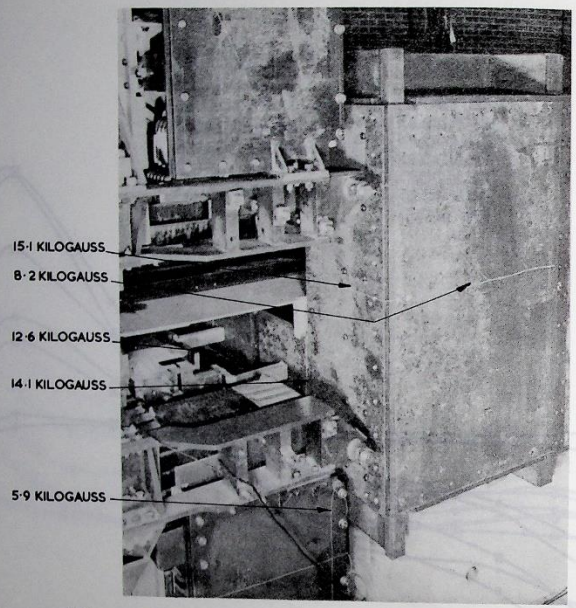

Fig. 4.4.1(i) Flux densities in straight section box.

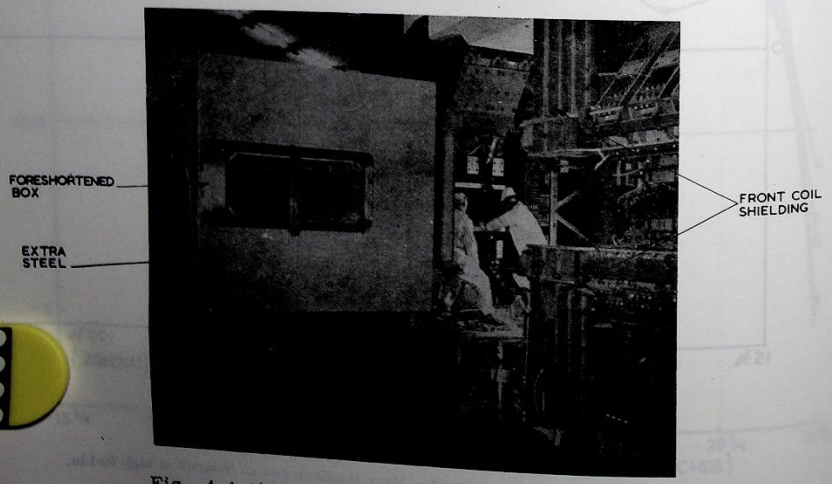

Fig. 4.4.1(ii) Straight section box and coil shielding.

4.4. Straight Sections

In the design of the straight sections and octant ends, the magnetic fields can no longer be taken to be two-dimensional. The design had to ensure:

(i) That the field in the straight section would be reduced to such a value that it would not have too much effect on secondary beams scattered from a target near a straight section

(ii) That the field from the magnet would not decrease the permeability of the ferrite in the r.f. accelerating cavity and that the ferrite would not distort the magnet field shape

(iii) That the effective length of the octants would be as near to the theoretical length as possible at all field levels

(iv) That the field shape at all field levels would be reasonably correct.

The three main components of the straight sections are straight section boxes, coil shielding and end pole-pieces. The following designs were established using Model III(8) and Model VI(11). Model VI had the same coil configuration as the main Nimrod magnet.

4.4.1. Straight Section Boxes

There was some distinction between the long (14 ft) and short (11 ft) straights. The design of the long straight boxes was dictated mainly by the requirements of the r.f. cavity; the inflector box was the main influence on the short straights. To provide good shielding of the straights mild steel boxes were chosen and the thickness of material required on the faces of the boxes was determined on Model III. Measurements of field gradients in the boxes showed that there was little difference in the field shape for the short and long straight cases. The flux densities measured on Model VI with a dummy r.f. cavity box with 2 in thick faces are shown in Fig. 4.4.1(i). In order to get scattered particles from internal targets as near as possible to the forward direction, the outside edges of the working ends of some of the boxes were cut back, the steel being replaced as shown in Fig. 4.4.1(ii).

4.4.2. Coil Shielding

The coil shielding is arranged to cut down the fringing flux from the main magnet coil and is shown in Figs. 4.4.1(ii) and 4.4.2(i). The flux densities as measured in Model VI are also shown on Fig. 4.4.2(i).

4.4.3. End Polepieces

End polepieces were designed using Model III and Model VI. Measurements on Model III were made to ensure that the effective length of the octant would be approximately correct and that it would not vary with field level. (Provided that all octants are the same length, an error in effective length of a few inches is permissible). A pole which was tapered azimuthally was used; to obtain optimum conditions, a taper into the second polepiece would be required. The resultant shape of pole was used on Model VI. By suitably subtracting effects due to the poles on Model VI, the effects on field shape of the ends of an octant were predicted. These are shown in Table 4.4.3(I).

TABLE 4.4.3(I)

Effective error in average 'n' due to octant end effects

Field (kilogauss)	Distance from outside of pole (inches)				
	16	18	20	28	30
10	.08	.13	.11	-.04	-.13
12	.11	.17	.13	-.09	-.24
13	.15	.19	.13	-.11	-.37
14	.16	.19	.13	-.11	-.47

It can be seen that this gives an appreciable error in n in the operating region. Some correction could be achieved by crenellating the end polepiece. A sample was made from $\frac{1}{4}$ in thick laminations with crenellations as shown in Fig. 4.4.3(i) and measurements on Model III (see Table 4.4.3(II)) indicated that it was worthwhile using crenellations on the end polepiece.

TABLE 4.4.3(II)

Effective correction in average 'n' due to end polepiece crenellation

Field (kilogauss)	Distance from outside edge of polepiece (inches)					
	16	18	20	26	28	30
8	.04	.02	.01	0	0	-.01
10	.04	.02	.01	-.01	-.02	-.03
12	.05	.05	.03	-.03	-.06	-.07
13	.05	.06	.03	-.03	-.07	-.08
14	.08	.06	.04	-.03	-.07	-.10

4.4.4. Overall n-correction

By adding the effects predicted from 28 pairs of Mark I poles, 12 pairs of Mark II poles and the end effects, an overall average n-value for an octant was obtained (Fig. 4.4.4(i)). The values obtained during the survey are shown in Fig. 4.4.4(ii). The main difference in the predicted and measured values is at the inside of the good field region and is due to the greater correction of the Mark II poles mentioned in Section 4.3.

At low fields the effective n at the inside radius at the end of an octant was always high, even without inner shims on the end polepieces. This is because

Fig. 4.4.2(i) Coil shielding.

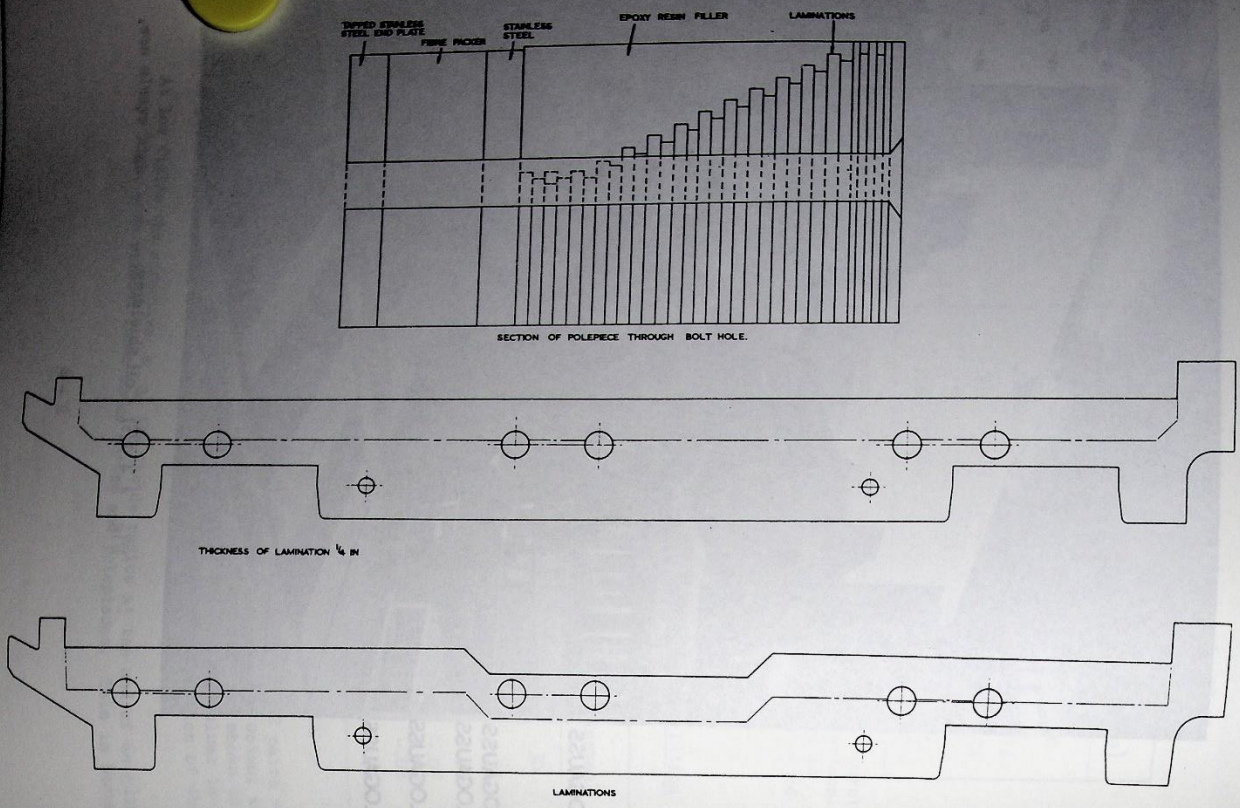

Fig. 4.4.3(i) End polepiece.

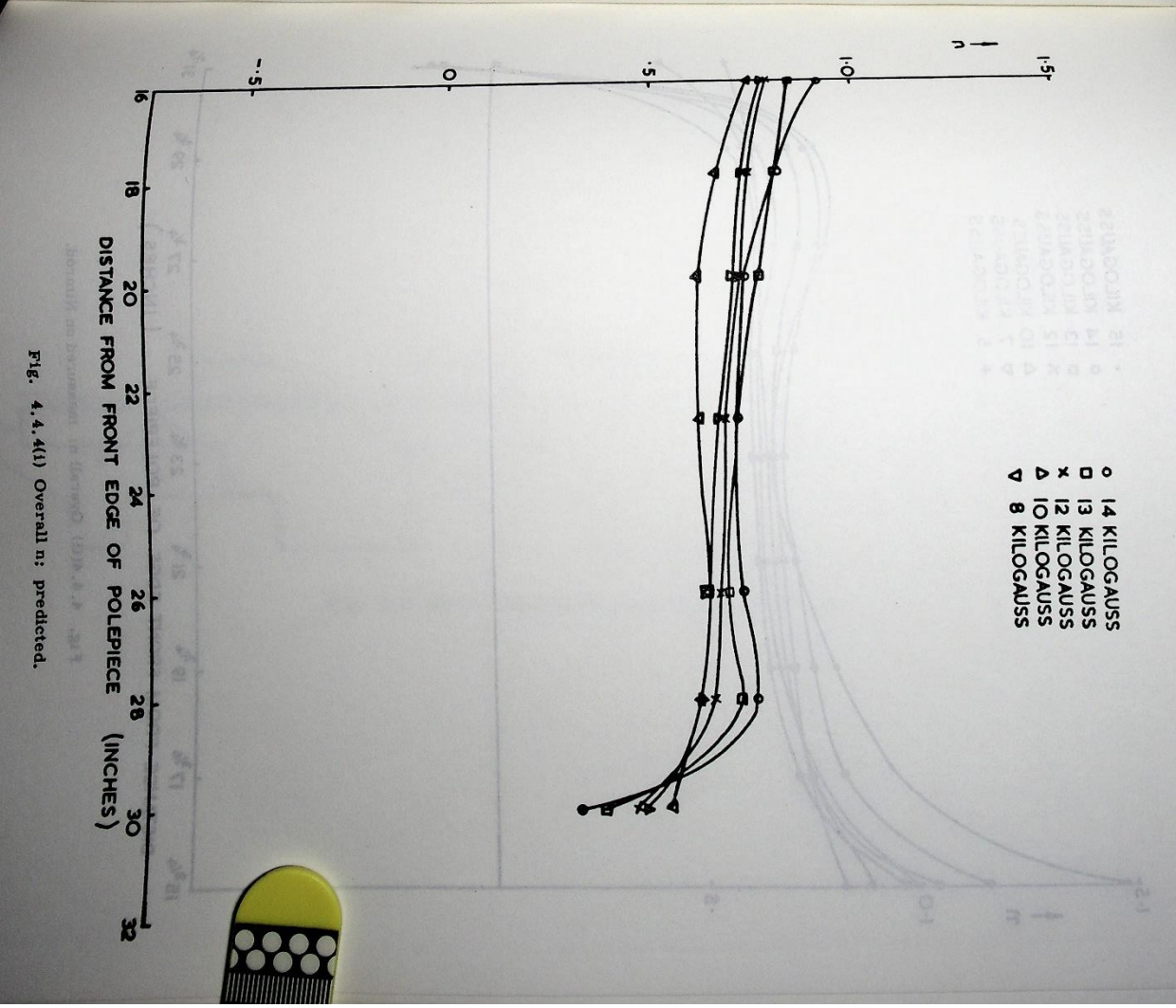

Fig. 4.4.4(i) Overall n; predicted.

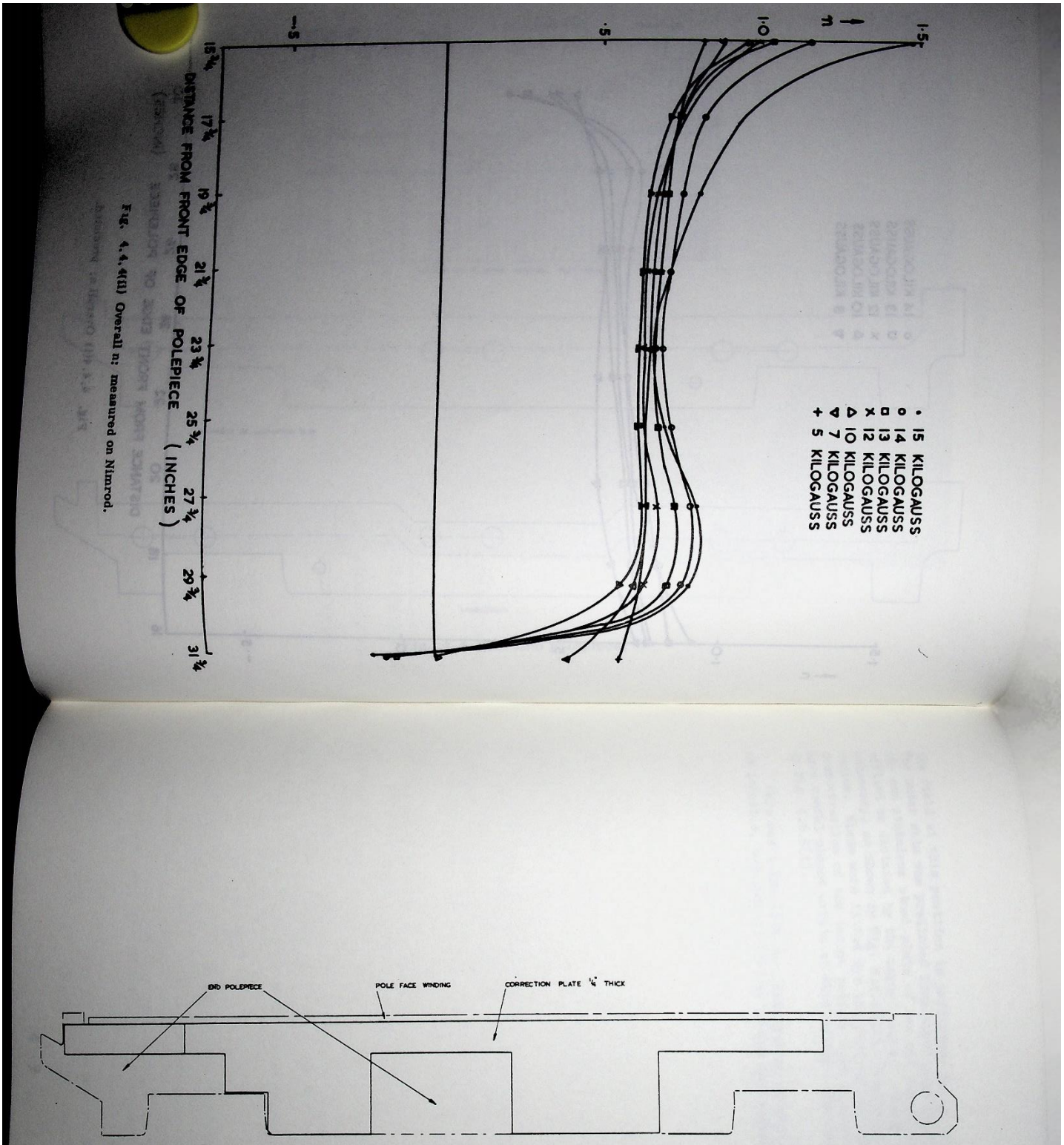

Fig. 4.4.4(ii) Overall n: measured on Nimrod.

Fig. 4.4.4(iii) Correction plate on end polepiece.

the field at this position is influenced mainly by the presence of the gap coils. The outer shim was predicted from model measurements. Tapped holes were drilled in the end stainless steel plate of the end polepiece to enable correction plates to be affixed as dictated by the magnet survey. One $\frac{1}{4}$ in plate was found to be necessary, as shown in Fig. 4.4.4 (iii) due to an overcorrection at the outside radius. These were fitted for the rest of the survey. There was still overcorrection of the inside radius; this is not so important since particles do not have useful closed orbits at this radius. The overall low field n-values are shown in Fig. 4.6.9(i).

Care was taken with the installation of straight sections to ensure, as nearly as possible, constant conditions around the magnet ring.

4.5. Mechanical Alignment of Sectors and Polepieces

4.5.1. Requirements

The mechanical alignment of sectors and polepieces had to meet the following tolerances:

(i) The radial and azimuthal tilt of the polepieces must not exceed ± 0.001 in in 48 in and 13 in respectively

(ii) The mean plane (defined by the mid point in height between the poles) must lie within a 0.040 in wide band around the whole 150 ft dia. circle, with limitations on the number of lobes and steps between adjacent octants and sectors

(iii) All poles must be within 0.050 in of their correct radial position and the overall lengths of the octants must be correct to within 0.050 in with a limitation on changes between adjacent sectors.

4.5.2. Methods

The machine alignment was broken down into four stages:

(i) Stage 1 involved installation and survey of 24 floor reference points defining the machine geometry. These 24 points formed a network of 8 triangles and 12 quadrilaterals. They have been surveyed 8 times in plan and 32 times in height and the height surveys are continuing.

The survey plan and equipment was designed to ensure that the position of any one of the 25 points was known accurately to within ± 0.005 in. From the survey measurements plan coordinates were computed, the difference between computed coordinates and nominal coordinates showing the error of each datum point. Height differences were also subject to a least squares computation, the results giving the height of each point in relation to the datum.

The surveys have shown that the plan position of any one point is known to within 0.008 in and its height to within 0.002 in at a confidence level of 95%

(ii) Stage 2 consisted of setting datum screws and marks on the 336 magnets defining the features which were to be accurately aligned. Since the gap of the magnets which faced outwards was the only part machined and, for all practical purposes, there was no gap between sectors at the inner dia., it was necessary to define and reproduce datums at the rear and on top of the sectors which could be seen and measured from the octant centre. This operation became almost a production exercise with each sector having its datums set in relation to its characteristics in a measuring station.

(iii) Stage 3 was the alignment of magnets in relation to the floor reference points. In each octant, six sectors, approximately equally spaced, were positioned by tape and theodolite using special purpose ancillaries. Heights and tilts were obtained using a surveyor's precise level. These principal sectors, when positioned, were used as references to "fair in" the remainder. For this a special large steel beam was used with a measuring station jig bored for each sector position.

Sector alignment was completed in four months and when complete the heights

of all 336 sectors lay between limiting planes 0.02 in apart. The instruments and methods used were capable of greater accuracy the larger part of the error being due to movements of the foundations.

(iv) Stage 4 was concerned with polepiece alignment and was a temporary installation without the vacuum vessel in place to allow the magnetic survey to be carried out.

All these stages were preparatory to the final task of aligning the polepieces inside the outer vacuum vessels within the limits stated above. This final installation took ten months (working 12 hours per day, seven days a week) and was completed at the end of January 1963. The reference marks on the front of the sectors were used as datums for polepiece positioning, a pair of poles was installed in each principal sector and the remaining pairs faired in. Heights and tilts were controlled optically, direct from the survey height datums. A considerable amount of special lifting, handling and alignment gear was designed for this operation, which was carried out under clean conditions.

4.5.3. Results

The alignment achieved is shown in Fig. 4.5.3(i). Table 4.5.3(I) relates these results to the original specification.

TABLE 4.5.3(I)

Tilts. Radial and asimuthal.		
Specified: ± 0.001 in	Achieved:	50% of all poles within ± .001 in
		80% " " " " ± .002 in
		95% " " " " ± .003 in
Plan Radial position.		
Specified: ± 0.05 in	Achieved:	all sectors within ± 0.010 in
		all poles (in relation to sectors) within ± 0.005 in
All sectors lay on their correct radius within ± 0.005 in		
and polepieces are correct to sectors within ± 0.003 in		

4.5.4. Foundation Movement

The main reason for the poor results in height was foundation movement. For various reasons it was not possible to complete the earth mounding on the roof, which forms part of the biological shielding, until the polepiece installation programme was more than one third complete. The effect of the mounding has been to "bend" the monolith. It has been shown that the addition of 100 tons is the equivalent of 0.001 in deflection, not always however in the place most expected. "Spring back" when loads are removed appears to be very much less, perhaps less than a quarter of this figure.

Since the thermal co-efficient of the monolith is approx 7 x 10^{-6}/°C small

temperature gradients can cause dishing. Some dishing is also caused by the columns carrying the roof.

Temperature fluctuations of approximately 1°C are normal and probably account for the change in height of floor datums when they are measured monthly. These height measurements show a flutter of about ± 0.005 in in a random fashion month by month. Tilts also vary by about the same amount and it is unreasonable to expect the monolith to be more stable than this with the existing temperature controls.

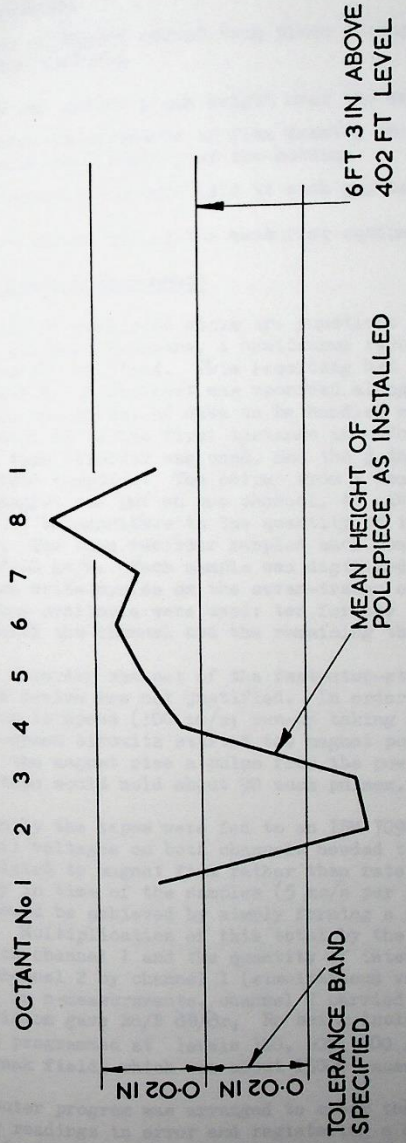

Fig. 4.5.3(i) Diagram of heights, showing alignment achieved.

4.6. Magnetic Survey

The survey of Nimrod magnet took place during the period April-August 1962. The measurements included

(i) n-values and median plane height over the entire working area of the machine

(ii) comparative measurements of flux density on the equilibrium orbit radius (Ro) to examine the symmetry of the machine

(iii) measurements of the end-field at each gap between adjacent octants.

A detailed report (4) of the measuring equipment has been published.

4.6.1. Pulsed Field Measurements

The quantities mentioned above are functions of the instantaneous field level in the magnet gap and therefore, a continuous recording during the rising part of the field pulse was required. This recording had to be a two-channel one, whereby the magnet quantity of interest was recorded alongside an indication of the field level. Because the amount of data to be handled was large, it was decided to attempt to record it in the first instance in a form acceptable to a computer. A two-channel tape recorder was used, and the $\frac{1}{2}$ in tape produced was compatible with the IBM 7090 computer. The output from a search coil in a "standard position" on Ro in the magnet was put on one channel, to give the field level and a search coil designed to be sensitive to the quantity of interest was connected to the other channel. The tape recorder sampled each search coil voltage alternately at a frequency of 10 kc/s. Each sample was digitized into a ten-bit number which was recorded in two write-cycles on the seven-tracks of the tape. The fourteen bits per reading thus available were used: ten for the digitised reading, one for a label to indicate the channel and the remaining three for parity-checking bits.

The tape recorder was not of the fast-stop-start variety, because the extra cost of such a device was not justified. In order to record a magnet pulse, the tape was run up to speed (100 in/s; run-up taking about 1 s) and then a pulse from the tape-speed circuits started the magnet pulse and also the record circuits. At the end of the magnet rise a pulse from the power supply timer stopped the recorder. A tape would hold about 90 such pulses.

Subsequently the tapes were fed to an IBM 7090 to process the information. The search coil voltages on both channels needed time-integration to arrive at quantities related to magnet flux rather than rate of change of flux. Because of the density in time of the samples (5 kc/s per channel) a sufficiently accurate integration could be achieved by simply forming a running total of the samples in the computer. Multiplication of this total by the appropriate constants gave the flux density on channel 1 and the quantity of interest on channel 2. In all cases, division of channel 2 by channel 1 (simultaneous values) gave a meaningful result. (For example; in n-measurements, channel 2 carried field gradient information $\partial B/\partial r$, so division gave $Ro/B\ \partial B/\partial r$, Ro being included in the multiplying constants). Print-out was programmed at levels 300, 600, 900 and then every multiple of 1000 gauss up to peak field, which was about 15000 gauss.

The computer program was arranged to check the parity of the readings, rejecting any readings in error and registering a count of errors of various types. To eliminate drift of the zero-input reading of the recorder, use was made of the

interval between the initiating pulse and the magnet coming on, to establish a zero in the computer based on the actual recordings in the two channels. This zero was then used for the rest of that record and printed out at the end. Provision was made for setting up a four-figure identity which could be written automatically at the start of each record, before sampled voltages were recorded. The identity bits were written three times at the start of the record, which thus characterized a true record from any spurious bits which could be interpreted by the computer as a record. The sensitivities available were 40 mV up to 20 V in independent switched ranges on channels 1 and 2. The zero could be located either at the negative end of the voltage range, or half way, catering for unidirectional or bidirectional inputs.

4.6.2. Remanent Measurements

The remanent field in the magnet was about 8 gauss, an appreciable fraction of the injection field, 300 gauss, and therefore arrangements were necessary to survey the remanent field. In most cases this was done by moving a search coil in the field and integrating the resultant e.m.f. in an optical servo type fluxmeter, to give the flux change. The fluxmeter readings were recorded by a digital voltmeter, and both printed and punched on paper tape which was processed in a Ferranti Mercury computer. An exception to this method of measuring was the remanent median plane survey, where a fluxgate saturating strip magnetometer probe was used. For both the pulsed and steady field measurements, the search coils were located on paxolin trolleys and moved by compressed air cylinders. Rotation of the coils was achieved, when necessary, by use of paddle-type air-driven actuators. The search coils were formed on ground-marble formers and bonded with marble dust loaded resin.

4.6.3. n-measurements

The field index, n, was measured with an opposed coil-pair, sensitive to gradients, and not to uniform flux.

The n-values were taken at 2 in radial intervals and 3 sector (about 40 in) azimuthal intervals, all round the machine. The coil-pair was arranged to be 3 sectors long, so that all the machine area was covered. The n measurements were taken to an accuracy of about three decimal places.

4.6.4. Machine Symmetry Measurements

The flux-measuring search-coils used for these measurements were again 3-sectors long, and 2 in wide. In the pulsed field measurements a coil was placed in the standard position in the machine and connected in series opposition with an exactly similar coil which was carried round the machine. The computer program in this case was arranged to give percentage differences in flux density at the various machine locations, with an estimated accuracy correct to 0.001%.

The remanent comparison was made absolutely, to about 5 parts in 10^4, using a search coil which was turned over in the field, indicating the resultant flux change on a servo-flux meter. The machine symmetry measurements were made only in the octants, and stopped $4\frac{1}{2}$ sectors short of the ends.

4.6.5. Effective Length

The pulsed effective length was measured by placing a long coil of accurately known width on the Ro line at the end of the octants. This coil started at the point where machine symmetry measurements left off, i.e. $4\frac{1}{2}$ sectors from the octant end, and extended to the middle of the straight section. The coil was connected in series opposition to a flux coil in one of the standard machine positions and was of such a turns-area as to exactly oppose the long coil when the effective length of the end $4\frac{1}{2}$ sectors was equal to the geometric length.

For remanent measurements, a trolley carrying a search coil was arranged to follow the path occupied previously by the long coil described above. This search coil was indexed 2 in at a time and at each position the coil was rotated through 180^o and the fluxmeter readings recorded. The recording (on punched tape) was used to integrate the remanent flux density at Ro over the length of travel of the trolley.

4.6.6. Median Plane

In order to locate the median plane of a nearly uniform magnetic field, it is necessary to use a sensitive, direction-dependent, field-measuring device, which is capable of being orientated in the magnet gap with the position of its magnetic axis known very accurately. For instance, in Nimrod, with an n of 0.6, it can be shown that the curvature of the field lines in the gap is about 1000 in. To resolve a discrepancy of 0.1 in. between the geometric and magnetic median planes, therefore requires that the probe axis be angularly positioned better than 0.1 in 1,000, $\triangleq$ 20 seconds. If the vertical component of the field is B_z, the 0.1 in displacement results in a change 10^{-4} B_z in the horizontal field; which the probe must be able to measure. Since remanent field is about 10 gauss, 10^{-3} gauss must be measurable.

Position measurements were made optically. A plane vertical mirror was mounted on the probe carrier so that altering the inclination of the probes tilted the mirror about a horizontal axis. By obtaining an auto-collimating effect in a telescope with a gauss eyepiece, when the cross wires and their reflected image were coincident, the mirror was perpendicular to the axis of the telescope. With the telescope previously levelled the mirror would be in a vertical plane and the probe carrier would have some definite orientation relative to the vertical. The telescope used was an automatically levelled instrument incorporating a suspended prism. This equipment proved stable, robust and quick to use. Resolution of 2 seconds could be achieved with ease.

Fluxgate magnetometer probes were used to measure the magnetic field. These were 6 mm in length and were sensitive to 10^{-5} gauss. For the pulsed measurements a 3-sector long coil with a turns-area of 200 m^2 was mounted with its axis horizontal. Alignment was carried out in a subsidiary magnet, whose field was fairly uniform and approximately vertical. In the remanent case the horizontal field component in the geometric median plane was recorded, one probe after another being displayed by means of a multiway switch. In the pulsed case, the computer print out was of radial field in the geometric median plane, expressed as a percentage of main vertical field.

To do straight section measurements of remanent median plane, an aluminium bridge was used to carry a row of probes through the straight section box. A levelling mirror was provided on each end. Examination of the pulsed median plane in the straight section boxes was not attempted.

4.6.7. Other Miscellaneous Measurements

By arranging a large board horizontally in the end of an octant and halfway into the associated straight section box, readings were taken of the field in the median plane. A 6 in reference grid was used for positioning, pulsed readings being taken on the tape recorder and remanent readings with an gaussmeter and probe. Using a similar technique a field plot was taken moving radially away from the magnet in 6 in steps. This was done at two azimuths, corresponding to the Mark I and Mark II polepieces.

4.6.8. Results of the Survey

The survey has shown that there are no errors in the magnetic field shape which are not capable of correction with the available poleface windings and their supplies.

4.6.9. n values

The value of n as a function of field and radius is of prime importance in determining how much of the magnet aperture is usable. The average value of n over the whole machine, including straight sections, for various field levels is shown in Fig. 4.6.9(i). The usable portion is increased by correcting windings; discussion of the variation of aperture with field will be deferred until the effects of the correction have been shown.

4.6.10. Machine Symmetry and Effective Lengths of Octant-ends

These results have been combined to obtain a comparison of the octant strengths. There is sufficient data to compare the octants only in pairs, since the initial part of the current waveform is not the same for all octants. Also it is difficult to buck out magnet ripple, which varies by 180° octant to octant, and correcting data is not available. The histograms of Fig. 4.6.10(i) show the relative levels of neighbouring octants at various fields. They are field levels in the hard-edged octant of the correct geometrical length($R_0 \pi/4$) calculated to give the same line-integral of vertical field as the actual octant, including its end-effects. The levels are expressed as a percentage of the reference field for each pair of octants. It can be seen that pairs of octants are similar to 0.1% (or better) in nearly all cases, and that the level relative to nominal field decreases by about 0.7% at high fields. This is due to the effective length of the end-field decreasing.

4.6.11. Median Plane Results

The median plane variations at 300 and 15000 gauss are shown in Fig. 4.6.11(i) and 4.6.11(ii). They have been averaged for each octant and expressed as the fraction Br/Bo where Br is the radial field in the geometric median plane at any point and Bo is the reference field. The signs have been chosen so that an upward displacement of the magnetic median plane is represented by a positive value of Br/Bo The general features do not change much with field level: there is a dip in the neighbourhood of octant 7 in the median plane, which otherwise is above the geometric median plane. The marked rise in Br on the outside edge of the magnet is similar to that found on the Cosmotron(12). The general level of the magnetic median plane is about 0.1 in above the geometric median plane.

Some local distortions of the median plane were found. One large shift of

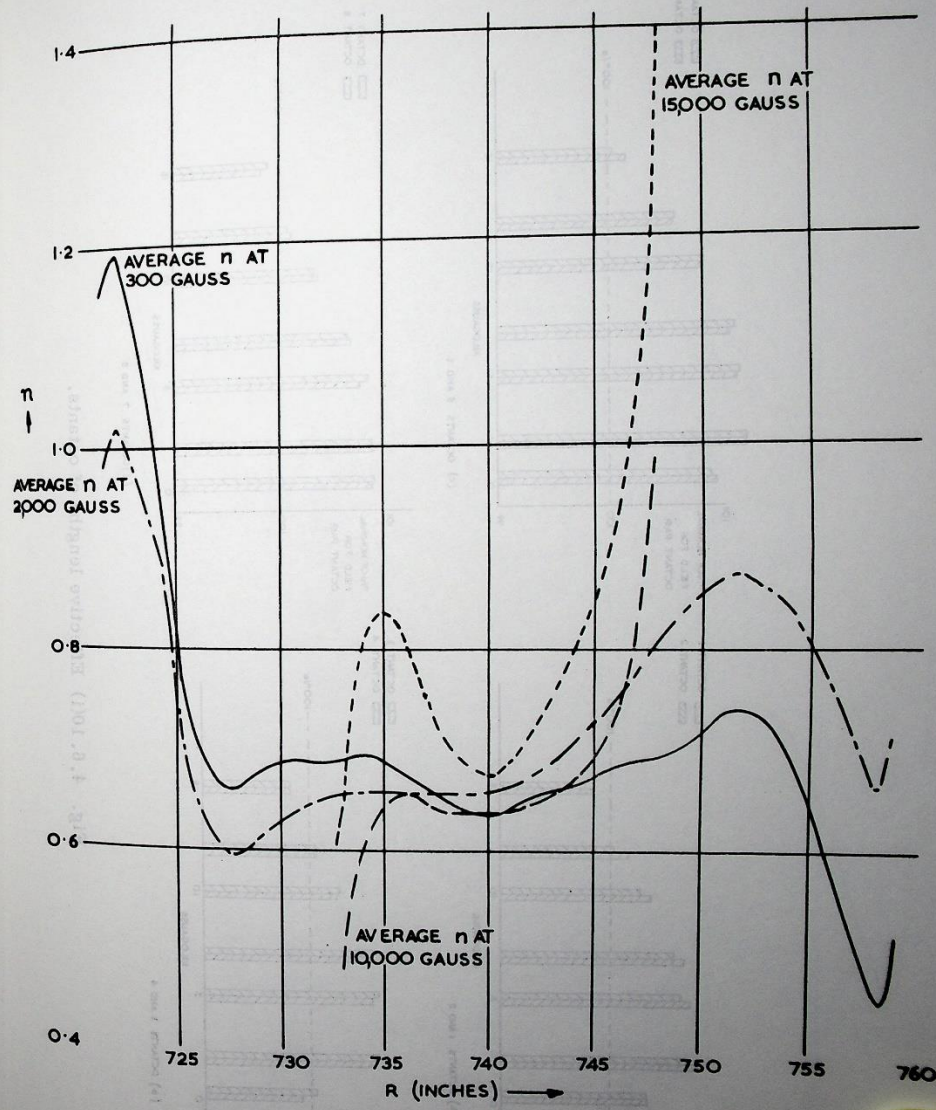

Fig. 4.6.9(i) Average n in Nimrod.

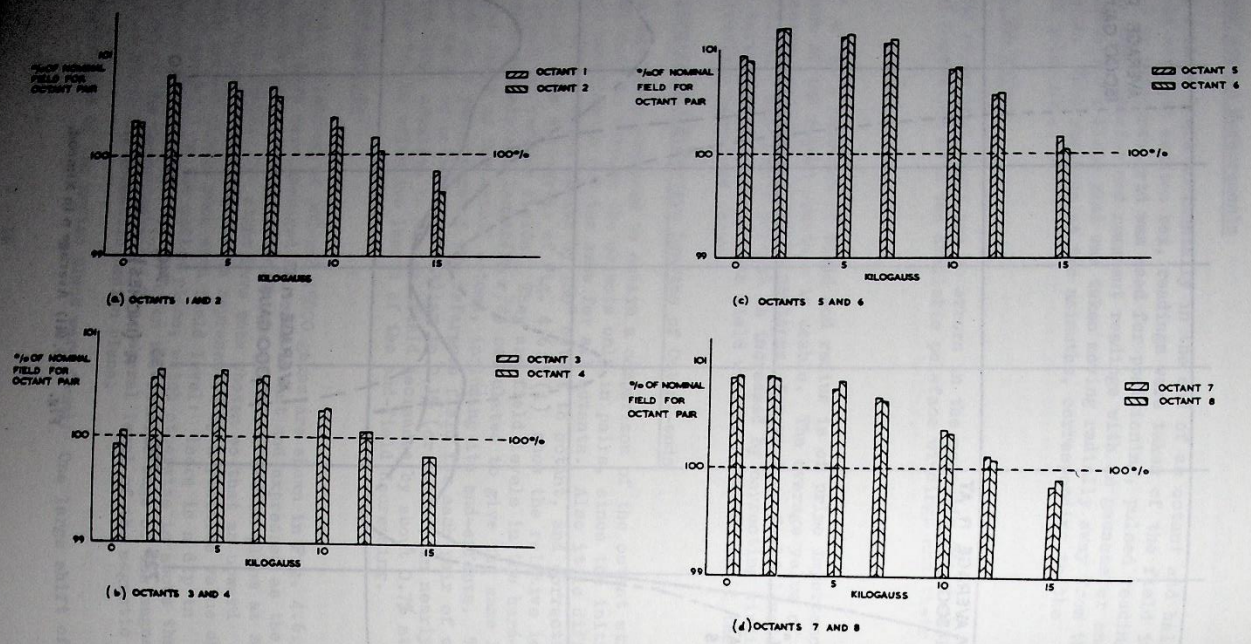

Fig. 4.6.10(i) Effective lengths of octants.

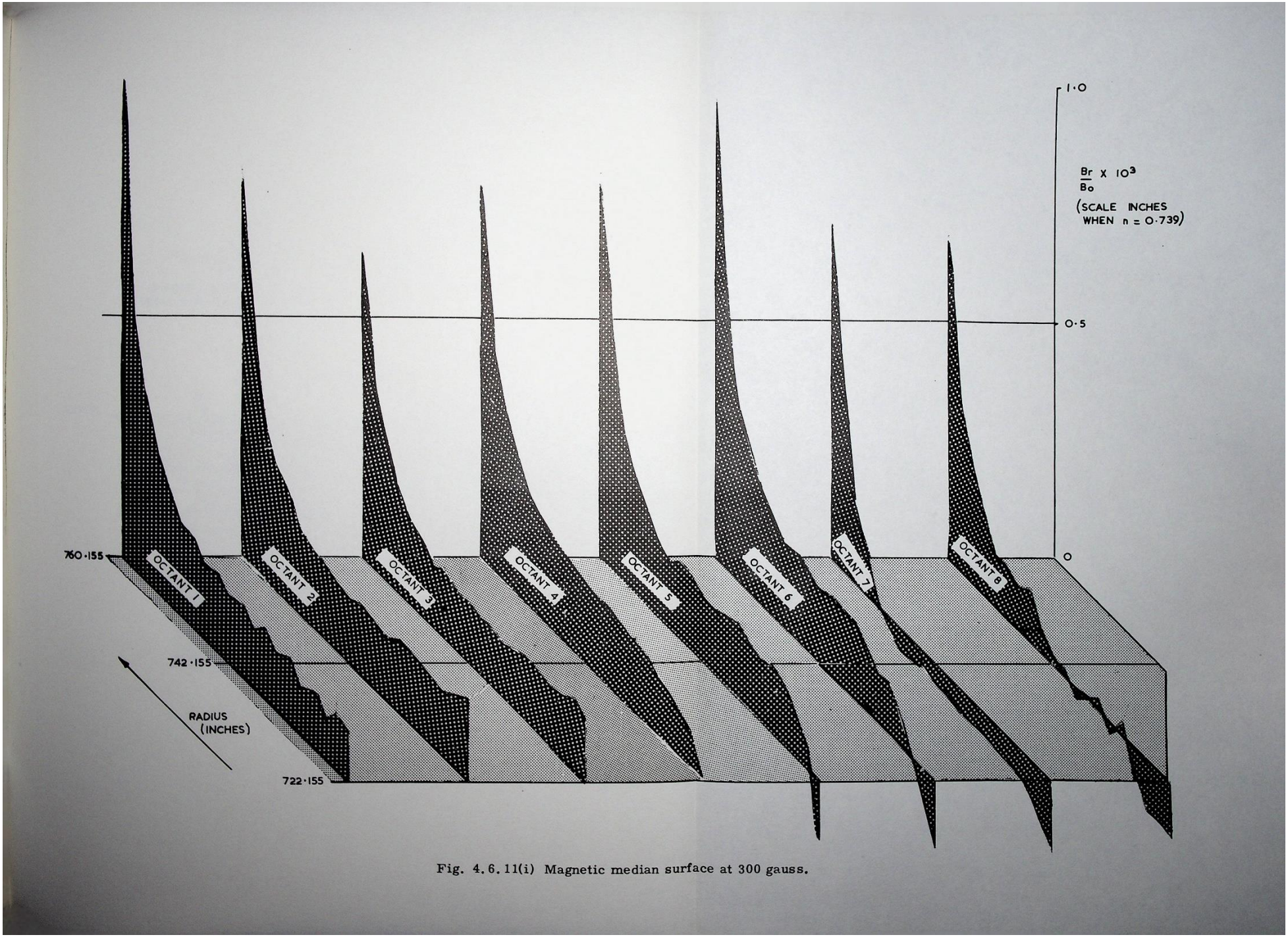

Fig. 4.6.11(i) Magnetic median surface at 300 gauss.

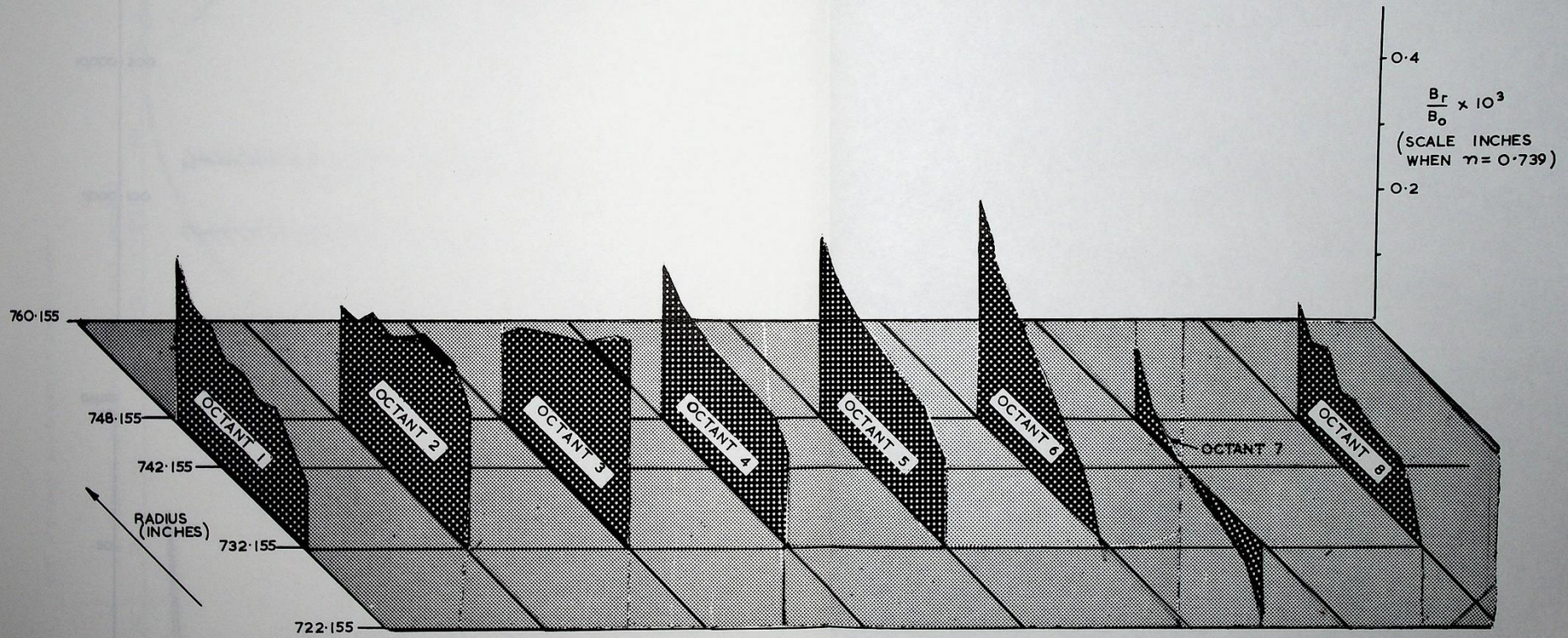

Fig. 4.6.11(ii) Magnetic median surface at 15,000 gauss.

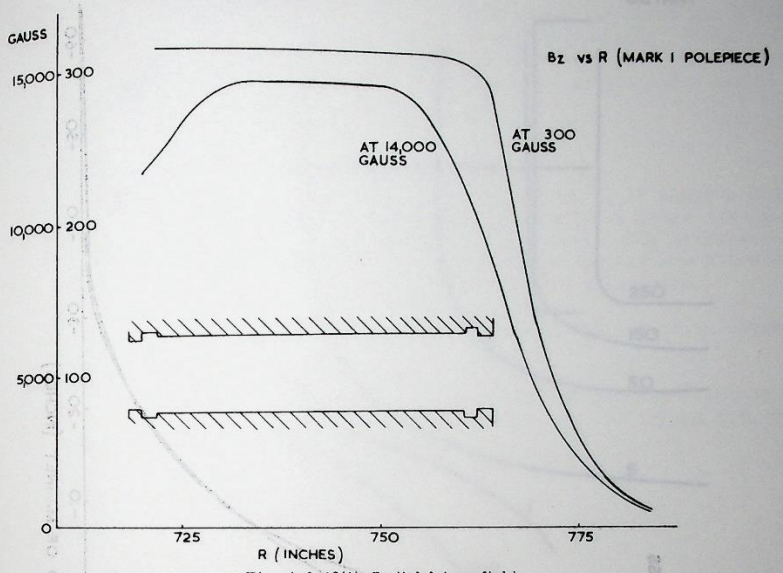

Fig. 4.6.12(i) Radial fringe field.

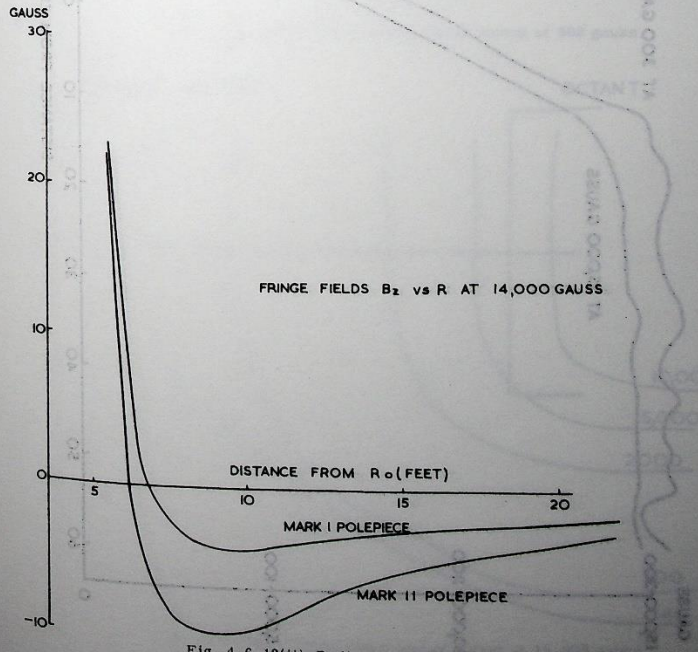

Fig. 4.6.12(ii) Radial fringe field at large distances.

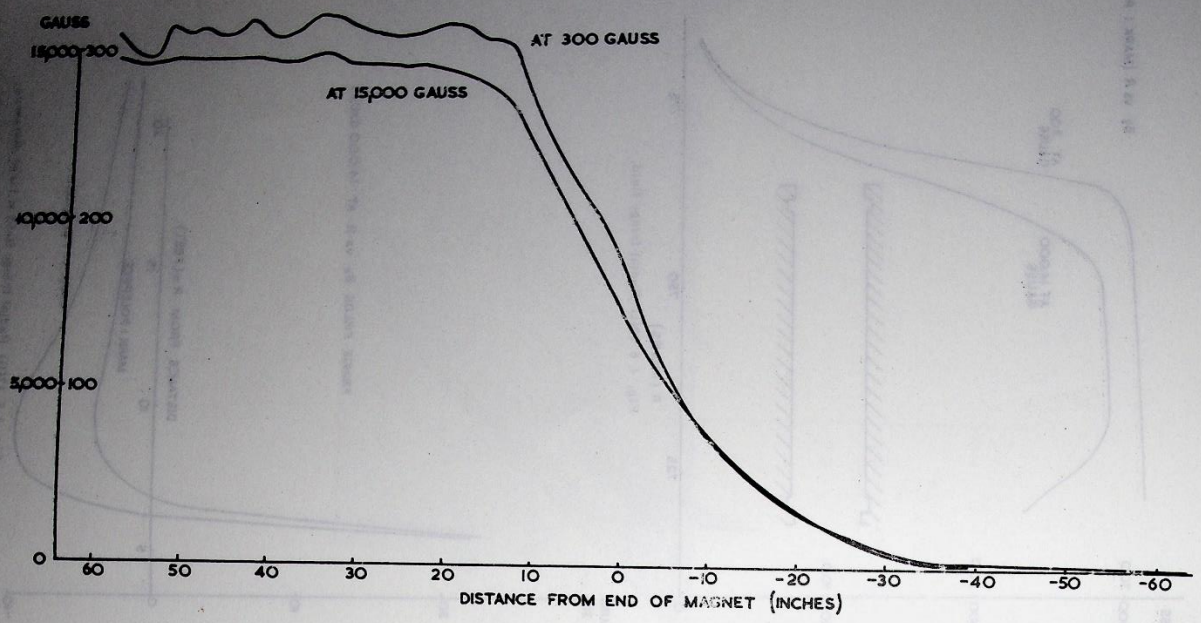

Fig. 4.6.12(iii) Fringe field into straight section.

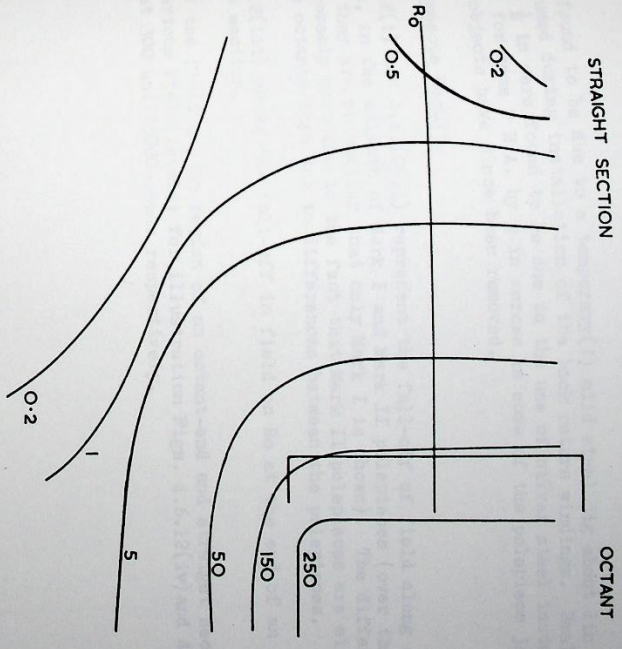

Fig. 4.6.12(iv) Field round end of octant at 300 gauss.

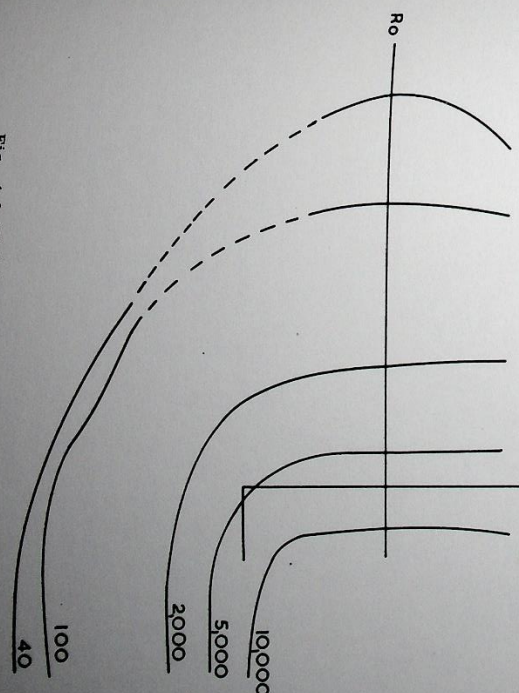

Fig. 4.6.12(v) Field round end of octant at 15,000 gauss.

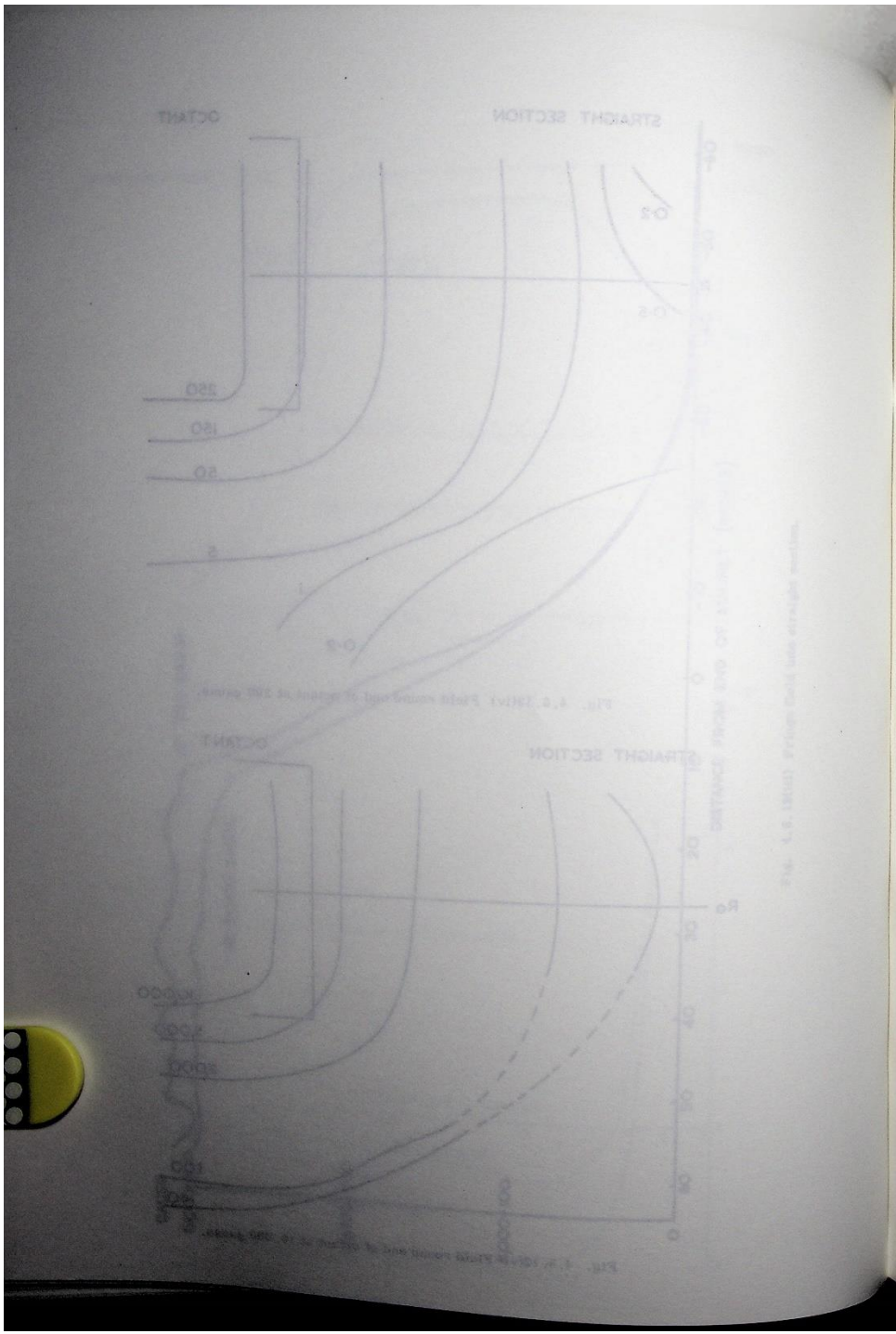

about 3 in was found to be due to a temporary(!) mild steel jig about 1in x 7in x $\frac{1}{8}$in which had been used during installation of the back return windings. Smaller shifts of about $\frac{1}{2}$ in were found to be due to the use of silver steel instead of stainless steel for some 2 B.A. by $\frac{1}{2}$ in screws in some of the polepiece jacks. The extraneous objects have since been removed.

4.6.12, Miscellaneous Results

Figs.4.6.12(i) and 4.6.12(ii) represent the fall-off of field along a radius from the magnet, in the azimuth of Mark I and Mark II polepieces (over the range of Fig. 4.6.12(i) they are so similar that only Mark I is shown). The differences in fall-off are probably more due to the fact that Mark II polepieces are situated at the ends of the octants than due to differences between the polepieces.

Fig. 4.6.12(iii) shows the fall-off in field on Ro at the end of an octant and in the straight section.

Mapping of the field in the region of an octant-end and straight section has been done at various field levels; for illustration Figs. 4.6.12(iv) and 4.6.12(v) show the maps at 300 and 15000 gauss respectively.

4.7. General Characteristics of the Magnet

4.7.1. Field Versus Current

The measured magnetic field and hence the proton energy of Nimrod for varying current is given in Table 4.7.1(I).

TABLE 4.7.1(I)

I (A)	B (kilogauss)	T (GeV)
2000	3.7	1.4
3000	5.6	2.4
4000	7.4	3.4
5000	9.3	4.4
6000	10.7	5.2
7000	12.1	5.9
8000	13.4	6.7
9150	14.6	7.3
10500	15.6	7.9
12000	$(16.4)^+$	$(8.3)^+$

+ estimated values

These are higher values of field than predicted in (1) due to the shaping of the poles (6) and the use of extra steel in crucial areas of the yoke (see Fig. 4.7.1(i)). These 'build-up plates' carry appreciable flux at high fields as shown by measurements on Model IV (Fig. 4.7.1(ii)). They also lead to a decrease in the remanent field in the magnet gap.

Calculations of rise times using predicted inductance or 'NA' figures have been confirmed in practice.

4.7.2. Eddy Current Effects

In addition to the normal depression of field due to eddy currents, (1),(7), (8) other eddy current effects become apparent when the control of flat-top slope was being investigated. The symptom was a very large transient depression (~.25 s) at the beginning of flat-top. Referring to Fig. 4.7.2(i), the curve XY gives the current expected from the impressed voltage on the magnet. The actual current obtained was on the path XZ. At high fields the size of the effect was much larger than the normal eddy current and hysteresis effect. Fig. 4.7.2(ii) shows the depression in current I_D as a function of rise time, i.e. peak current. Up to about 7,000 A the depression is constant at about 22 A and then rises sharply. The gap field in the magnet octant was depressed by an approximately constant amount as the rise time varied. Since a constant voltage is applied to the magnet and:-

$$V = NAdB/dt + RI \qquad .. \; .. \; (i)$$

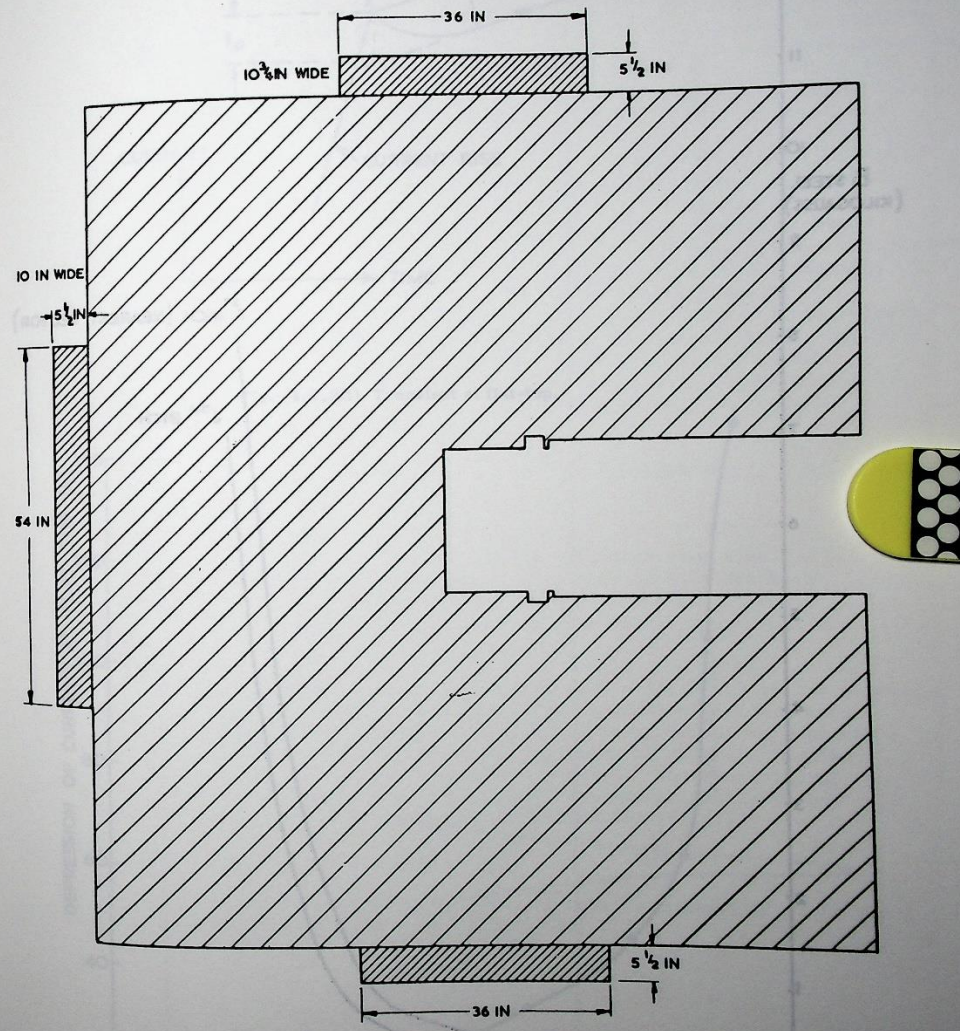

Fig. 4.7.1(i) Sector build-up plates.

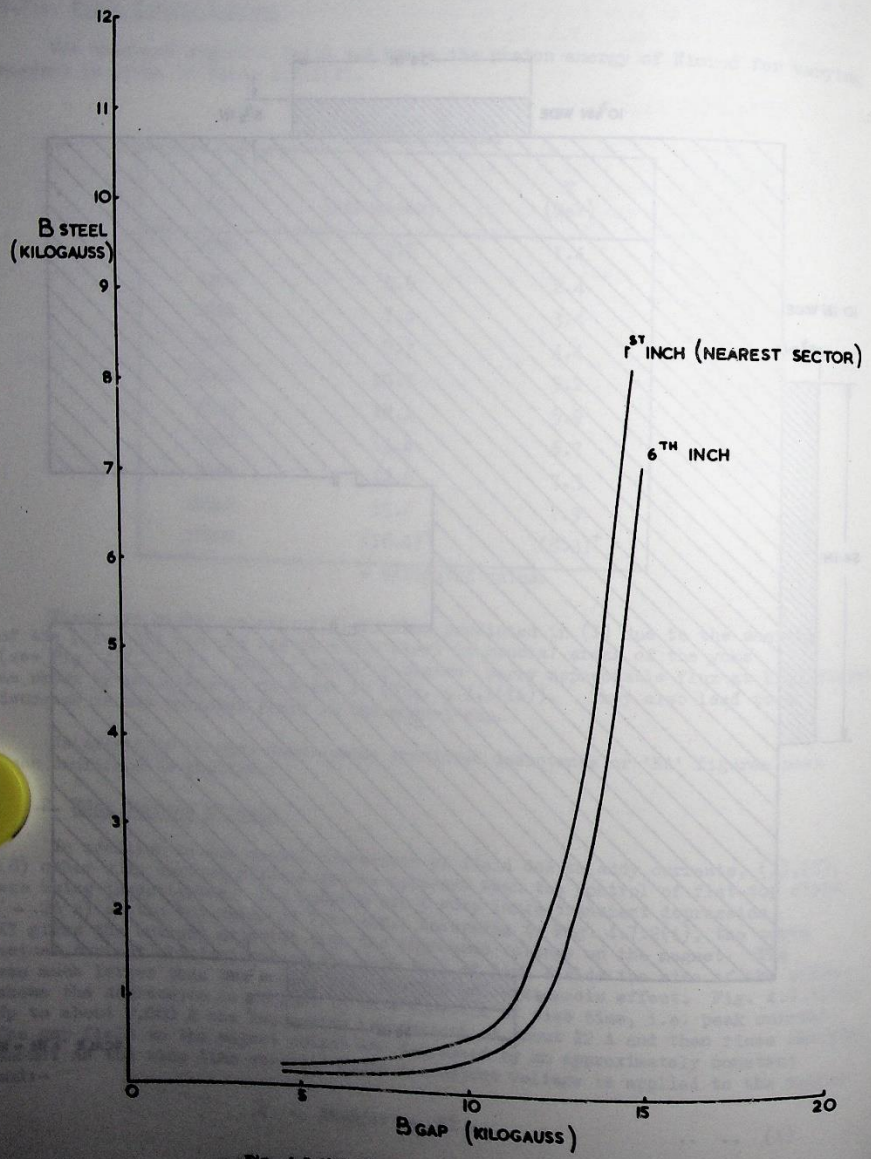

Fig. 4.7.1(ii) Flux density in build-up plates (Model IV).

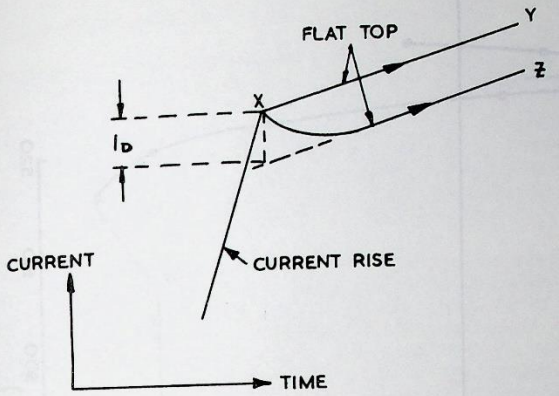

Fig. 4.7.2(i) Transient at flat-top.

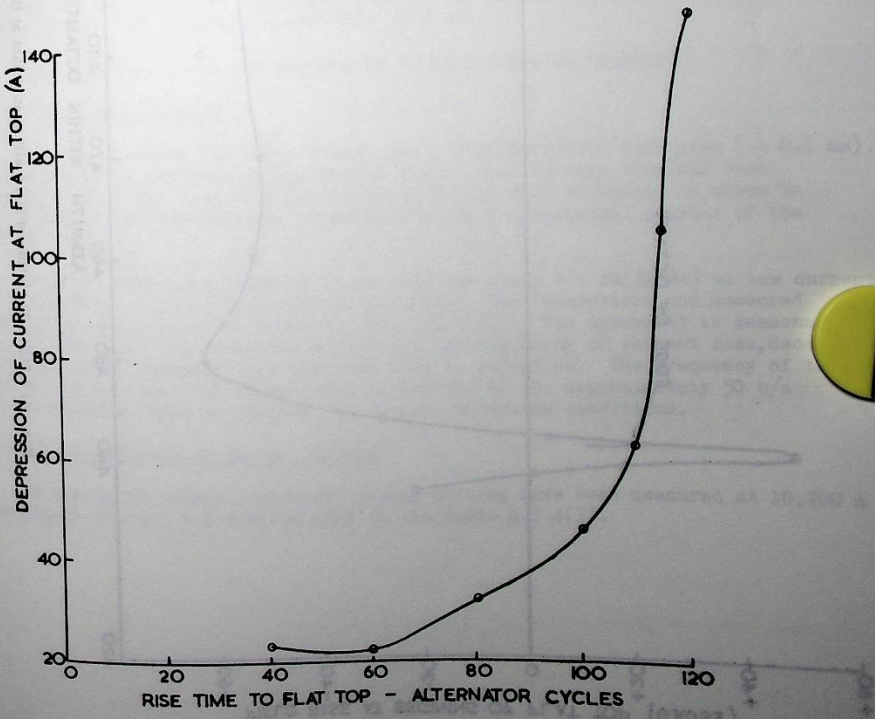

Fig. 4.7.2(ii) Depression of current at flat top with varying rise time.

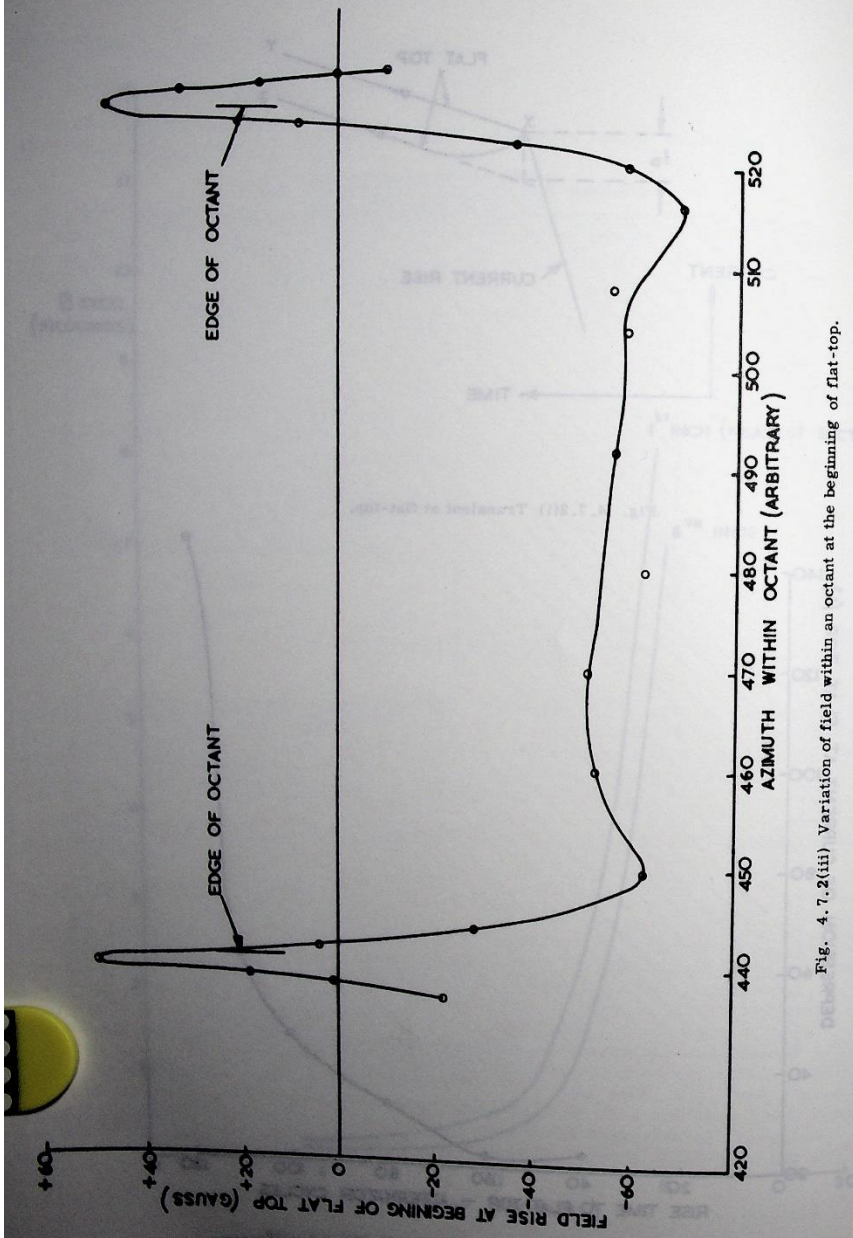

Fig. 4.7.2(iii) Variation of field within an octant at the beginning of flat-top.

there must be a redistribution of flux in the magnet.

Measurements of field depression azimuthally within an octant and straight section gave the result shown in Fig. 4.7.2(iii) showing a pronounced eddy current effect at the ends of octants at the transition from dB/dt on current rise to very small dB/dt on flat-top. This was the cause of the constant depression of field in the octant but did not explain the large depression in current at high peak currents. The eddy currents at the octant ends are due to fringe flux cutting the $\frac{1}{2}$ in end plates of the end sectors and also a $\frac{3}{4}$ in thick plate which was part of the coil shielding structure. This plate, which is thermally somewhat isolated, gets hot.

The high current effect was found to be due to the build up plates (Section 4.7.1). Measurements of the field just outside these showed a small value until the gap field reached about 10.5 kilogauss when there was a very rapid increase. This effect had also been found on Model IV; Fig. 4.7.1(ii) gives measurements of flux density in the build up plates versus gap field. Air gaps between the plates and the sector act as an impedance to flux until the sector starts to saturate, when there is a sudden increase of flux. Since the plates are laminated perpendicularly to the flux direction there are large eddy current effects. Again, from equation (i), since the total flux must remain at the correct value, as the eddy currents die away on going from current rise to flat-top, less current is required to maintain the flux and the current drops in the main magnet coils. Although the amount of eddy current power is quite considerable, no rise in temperature of the build up plates was detected.

Some correction for the depression in field will be required.

4.7.3. Transient Effects

The voltage from the power supply has a fast switch on rise time (~ 0.1 ms). The problem of transients in the magnet due to this voltage step has been discussed(13). The ring in magnet voltage due to this transient is shown in Fig. 4.7.3(i) for two adjacent octants, forming a symmetrical quarter of the machine.

By differentiating equation 20 in (13) and since V = NA(dB/dt) at low currents, the theoretical voltage transient is obtained. The theoretical and measured results for one octant are shown in Fig. 4.7.3(ii). The agreement is reasonable and confirms that the transient effects at the beginning of current rise, decay in a time short compared with the rise time to injection. The frequency of the oscillation is such that it will not be excited by the approximately 50 c/s voltage waveform used to produce the correct injection conditions.

4.7.4. Magnet Movements during pulsing

Movements of magnet components during pulsing have been measured at 10,700 A peak magnet current and are included in the Table 4.7.4(I).

TABLE 4.7.4(I)

Movements of magnet. (0.001 in).

Type of movement	Magnet component.	Sector Number. 42	41	40	39	38	37
CIRCUMFERENTIAL MOVEMENT (+VE INTO STRAIGHT SECTION)	SECTOR, TOP	+10	+8	+4	+1	+1	0
	P/P, UPPER (FRONT	+12	+8	+4	+3	+1	+1
	P/P, UPPER (REAR	+7	+4	+3	+1	0	0
	SECTOR, BOTTOM	+10.5	+6.5	+4	+2	+1	+1
	P/P,LOWER	+10.5	+6.5	+4	+3	+2	+1
RADIAL MOVEMENT (+VE WHEN OUTWARDS DURING PULSE)	SECTOR, TOP	+3.5	+3	+3	+3	+2.5	+3
	P/P, UPPER	+3	+2.5	+2.5	+2	+1.5	+1
	SECTOR, BOTTOM	+1.5	+.5	0	0	+.5	+1
	P/P, LOWER	0	0	+1	0	+.5	0
CLOSURE OF THROAT (UPPER POSITION: +VE DOWNWARDS) (LOWER POSITION: +VE UPWARDS)	SECTOR, TOP	+5	+10	+11	+11	+11	+11
	P/P, UPPER (FRONT	+7	+11	+12	+12	+11	+12
	P/P, UPPER (REAR	+3	+4	+5	+7	+5	+5
	SECTOR, BOTTOM	0	0	0	0	0	0
	P/P, LOWER	0	0	0	0	0	0

The movements recorded are all tolerable.

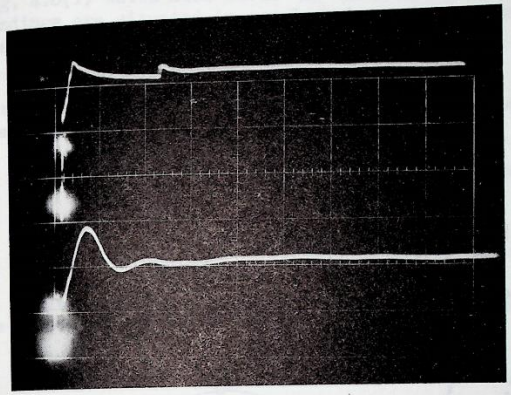

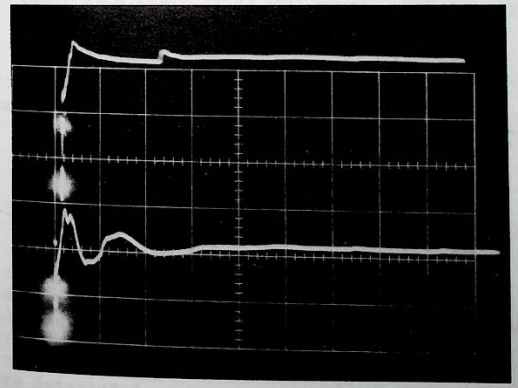

Fig. 4.7.3(i) Voltage transients at the beginning of current rise.

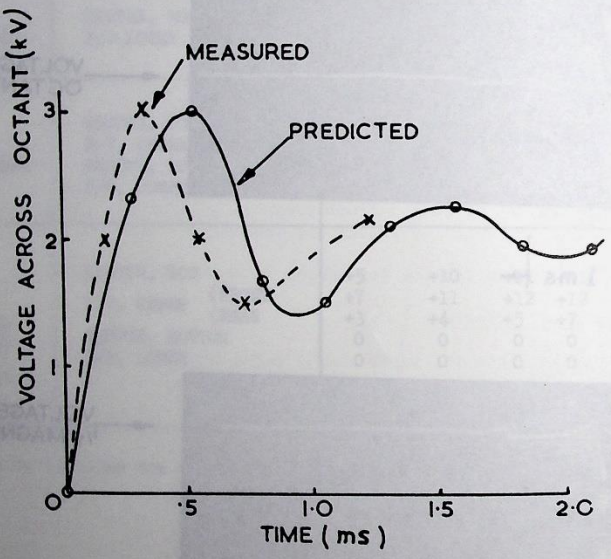

Fig. 4.7.3(ii) Measured and expected voltage transients.

4.8. Pole Face Windings

The dispositions of the windings with respect to the aperture are shown in Fig. 4.8(i) which also shows the function of each individual conductor. Return windings are situated in equal numbers on the inside and the outside of the aperture.

Consider a current +I to be passing through one pair of conductors (top and bottom): then the field gradient produced at the median plane is given by (see Fig. 4.8(ii)):-

$$\frac{dH}{dx} = \frac{\pi^2}{10g^2} \; I \; \mathrm{sech}^2 \; \frac{\pi x}{2g} \qquad \text{gauss/cm} \qquad (I \text{ in A})$$

$$= 0.0129 \; I \; \mathrm{sech}^2 \; \frac{\pi x}{2g} \qquad \text{gauss/in} \qquad (g = 5\tfrac{1}{2}\text{-in})$$

This assumes an infinite permeability for the iron and neglects the gap between the windings and the poleface.

For a current sheet top and bottom,

$$\frac{dH}{dx} = \frac{2\pi I}{10g}$$

or $$\frac{dH}{dx} = 0.09 \; I \text{ gauss/in} \quad (I \text{ in A/in})$$

Thus, at a field of 14,000 gauss, with R_o = 740 in, 100 A/in produces a change in n of: $\triangle n = \sim 0.45$

For current sheets in the opposite direction, there is no change in n , but a net radial component is produced which alters the level of the median plane by an amount:

$$\triangle z = \frac{560 \; I}{B_o}$$

4.8.1. Overall Adjustment of n and the Median Plane

Once the field has exceeded about 2000 gauss it is essential to short out of the circuit those conductors in the current sheets which are not in the good field region. Because of the inhomogenity of the field, large vertical forces would result on any winding carrying heavy current. In practice this means the removal from the circuit of the three conductors on the inside and the outside of the current sheet. This is achieved by switching as shown in Fig.4.8.1(ii), which is a more detailed description of the general circuit Fig.4.8.1(i). The octants are energized in pairs, so that the circuit of Fig. 4.8.1(i) is repeated for octants 2 & 3, 4 & 5, 6 & 7.

The 15 V, 5 A power units supply any current required during the injection period and up to a field level of about 1000 gauss. The current is then reduced quickly to zero, and switches A and C opened. The 60 kW supply is then brought into the

circuit by closing switches B and D. The e.m.f. induced in the windings is particularly troublesome because, although it has been minimised by juggling with return windings, during each acceleration pulse it reverses sign, as shown in Fig. 4.8.1(iii) and has a peak value of about 10 V per pair of octants.

Median plane adjustments are made with the 3.2 kW set, injecting oppositely directed current into the upper and lower layers. One set supplies the four pairs of octants in parallel.

4.8.2. Aperture at Injection

One 3.2 kW set will feed the whole magnet, the arrangement of connections being shown in Fig. 4.8.2(i). Considerations of available power and voltages induced in the windings by the rising field have led to a compromise arrangement whereby it will not be possible to make n quite as uniform across the aperture as was hoped. Four sets of windings are fed in parallel by the 3.2 kW set, these groups consisting of 2 and 25 Upper, 2 and 25 Lower, 4 and 23 Upper and Lower (in series), and 25 Upper and Lower. The currents are varied by means of rheostats in series with each group. To conserve current, 25 acts as the return conductor for 2, and 4 performs the same function for 23. These equal and opposite currents provide approximately the right correction to the field shape. Since conductor 25 lies at the outside of the aperture, the upper and lower windings have been placed in separate circuits so that the distortion in the median plane in this region may be corrected. The current arrangement is therefore as shown in Fig. 4.8.2(ii).

4.8.3. Aperture at High Fields

Because the current requirements for the windings at the inside and outside of the aperture are not the same, these windings have been placed in separate circuits (Fig.4.8.3(i)). This arrangement has the disadvantage that the same current must be passed through four octants at a time but the indications are that this lack of fine control will not be much of a drawback, as the field shape at high fields is fairly similar from octant to octant.

4.8.4. Bo Correction

Since it is not yet known what corrections have to be applied to B_o, no arrangements have been made apart from the provision of power supplies and four windings per octant.

4.8.5. Manufacture of Pole Face Windings

In each magnet octant there are two pole face windings, each continuous over the length of the octant; one is attached to the face of the upper set and one to the face of the lower set of pole pieces. The upper and lower pole face windings are housed in the interspace of the double walled vacuum vessel which is evacuated to a pressure of approximately 10^{-2} torr. Demineralised cooling water is passed through all the conductors of the pole face windings at a temperature of approximately 18°C.

Each winding consists of 26 conductors and 2 coaxial cables moulded within a glass fibre epoxy resin laminate. The following materials are used:

(i) Conductors – softened high conductivity tough pitch copper to BS.1037 with an electrical conductivity of not less than 98% I.E.C.

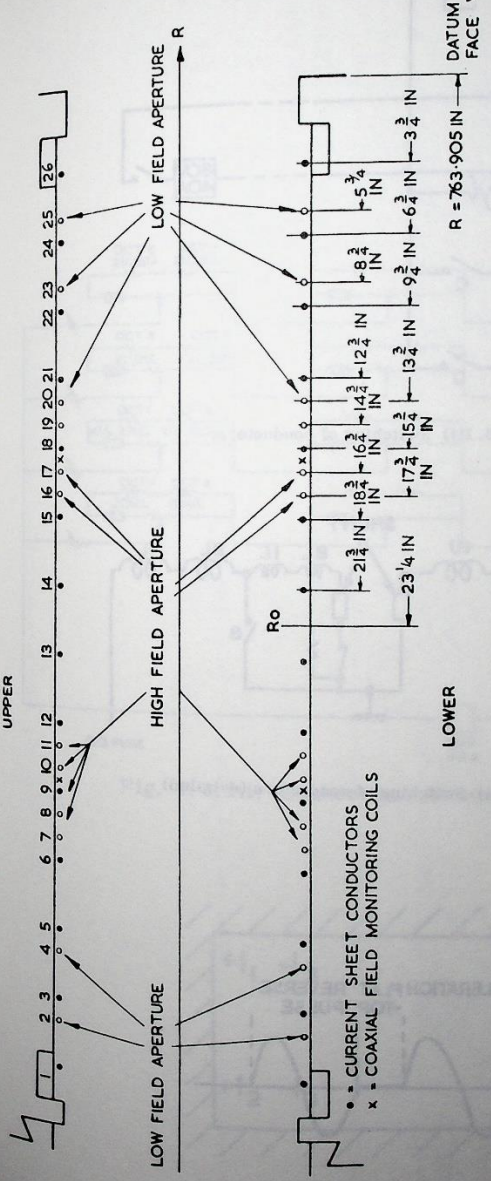

Fig. 4.8(i) Configuration of pole face windings.

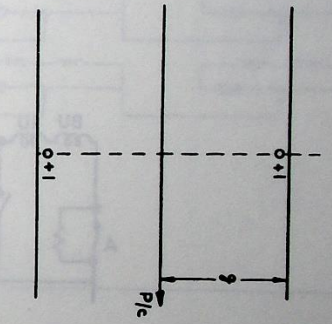

Fig. 4.8(ii) Diagram for winding calculation.

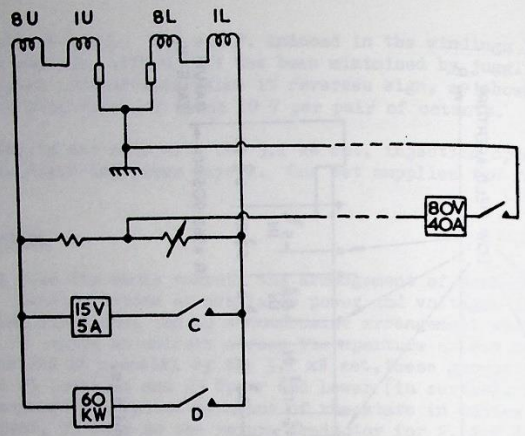

Fig. 4.8.1(i) Switching of conductors.

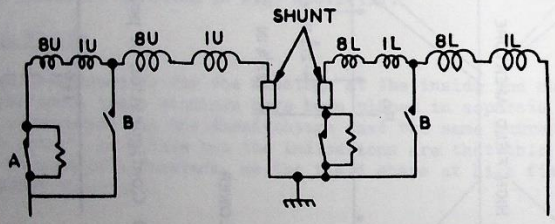

Fig. 4.8.1(ii) Switching of conductors (detailed)

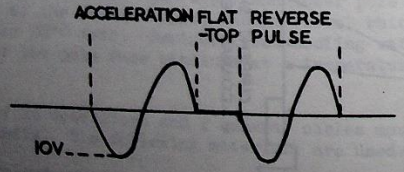

Fig. 4.8.1(iii) Voltage from n windings.

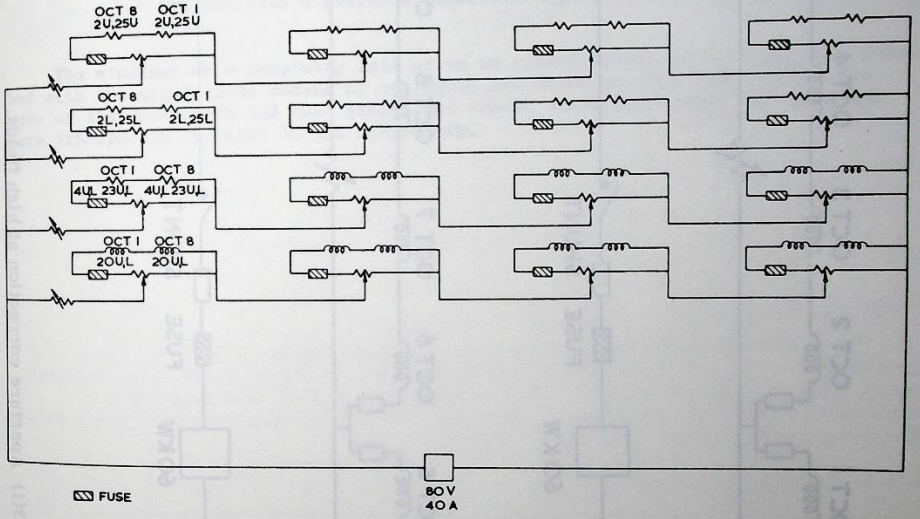

Fig. 4.8.2(i) Connections for aperture correction at injection.

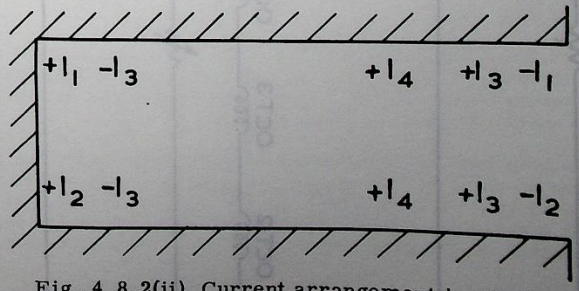

Fig. 4.8.2(ii) Current arrangement in windings.

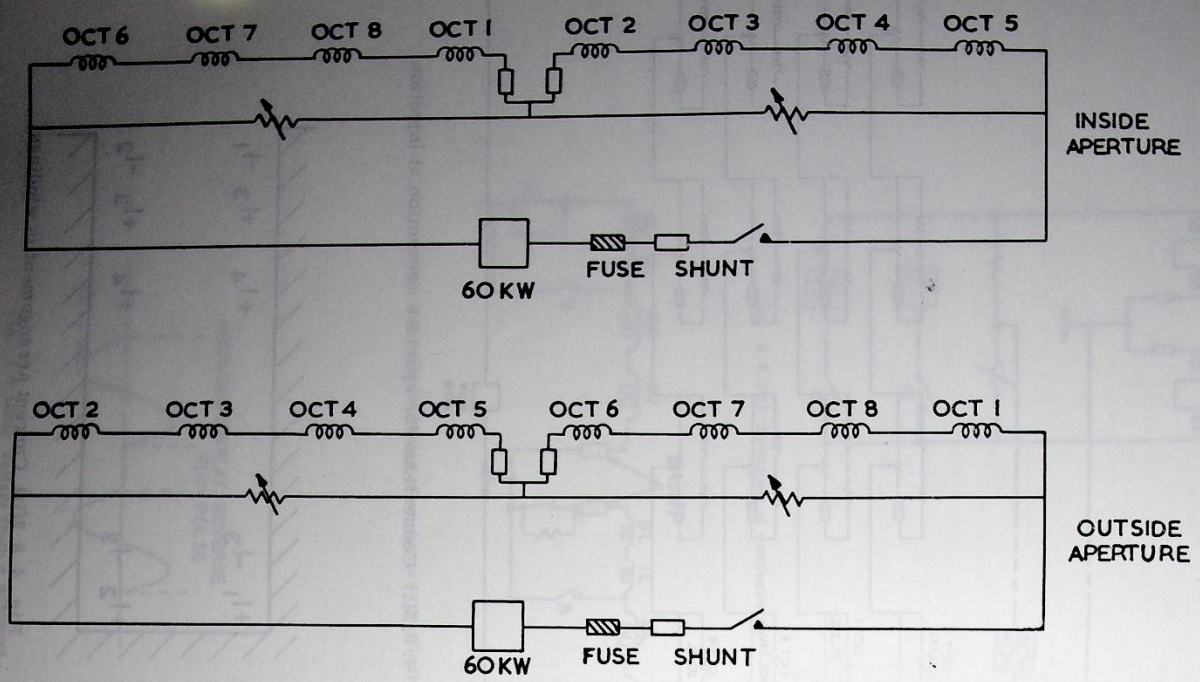

Fig. 4.8.3(i) Aperture correction at high fields.

and coated with polythene.

(ii) Laminate - outer skins top and bottom, 0.006 in glass cloth.
Main core glass mat - pre-impregnated.
Resin system: Araldite MY 470 - 100 parts by weight
Methyl Nadic Anhydride - 80 parts by weight
Ciba 33/1266 - 3 parts by weight
(Cure temperature 100°C ± 10°C for a minimum of 2 hours.)

(iii) Conductor End Terminations - phosphor bronze, silver brazed to the ends of the windings, insulated with a polythene sleeve and wrapped with a pressure sensitive impact adhesive polythene tape.

The windings were carefully laid up on an approximately 50 ft long mild steel bed with the appropriate radius of curvature and cured on this bed. After the ends of the conductors had been shaped and vacuum tests performed, the windings were transported in pairs to the Laboratory.

4.9. Pole Face Winding Power Supplies

The power supplies are of three types:

(i) 60 kW with a peak output of 400 V and 200 A.

(ii) 3.2 kW at 80 V, 40 A.

(iii) 15 V, 5 A.

4.9.1. Control Systems (General)

Each power supply has an associated control system which ensures that the currents through the pole-face windings are functions of the main field (B). The control systems are basically of the form shown in Fig. 4.9.1(i). The search coil is in the "good field" region of octants 5 and 6, and a voltage $V_1 = K_1B$ is induced in it when the main winding is pulsed. This voltage V_1 is integrated, producing $V_2 = K_2B$, and V_2 is operated on by a function generator to produce $V_3 = F(B)$. V_3 is fed into input 1 of a differential amplifier which is part of a closed control loop. The voltage (Vs) developed across the manganin shunt S, is fed into input 2 of the differential amplifier and the polarities of the inputs are arranged so that the output voltage from the differential amplifier is $G(V_3 - V_s)$, where G is the gain of the amplifier. The voltage $G(V_3 - V_s)$ is the control signal for the power supply and therefore the current through S is a function of B, to an accuracy dependent upon G.

4.9.2. Integrator Unit

A schematic diagram of the integrator is given in Fig. 4.9.2(i). Three integrators with different time constants are used, the amplifiers being Philbrick units. The feedback capacitors are shorted at the end of each pulse by a monostable multivibrator triggered from the end of the magnet current timing pulse. The integrator unit has been made and commissioned.

4.9.3. Function Generator

There are 13 function generators, one for each power supply. A schematic diagram is given in Fig. 4.9.3(i). The generator is a 10 point device which accepts a voltage proportional to the magnet field and converts to a voltage which is sufficiently finely controllable to be a specified function of the field. All 13 generators have been made and set up in the main control room.

4.9.4. 60 Kilowatt Supplies

The basis for these six units is a standard commercial 6-anode mercury arc rectifier set with transistorised grid control. This has a linear characteristic of output volts versus input control volts. The control and driver unit which is required for the supply is shown in Fig. 4.9.4(i).

All six sets have been delivered and are being installed. One set has been successfully operated under actual operating conditions with a full servo loop. Ripple at 300 c/s is reduced by a static choke-capacitor filter. At a current of about 150 A, 50 c/s ripple, which is inherently produced in the supply, is too great but modification of the grid control circuits should cure this.

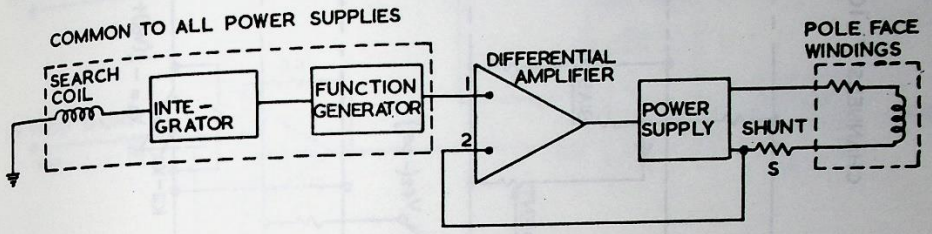

Fig. 4.9.1(i) Control system for pole face windings.

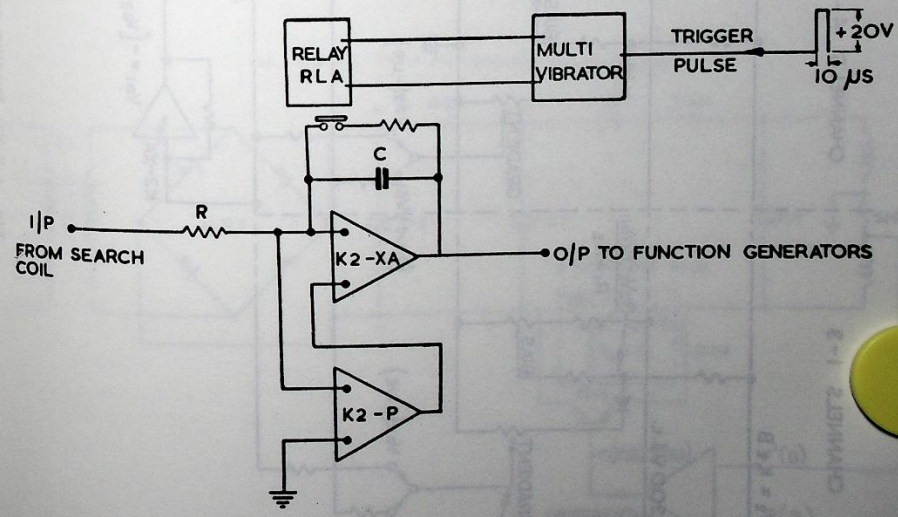

Fig. 4.9.2(i) Integrator.

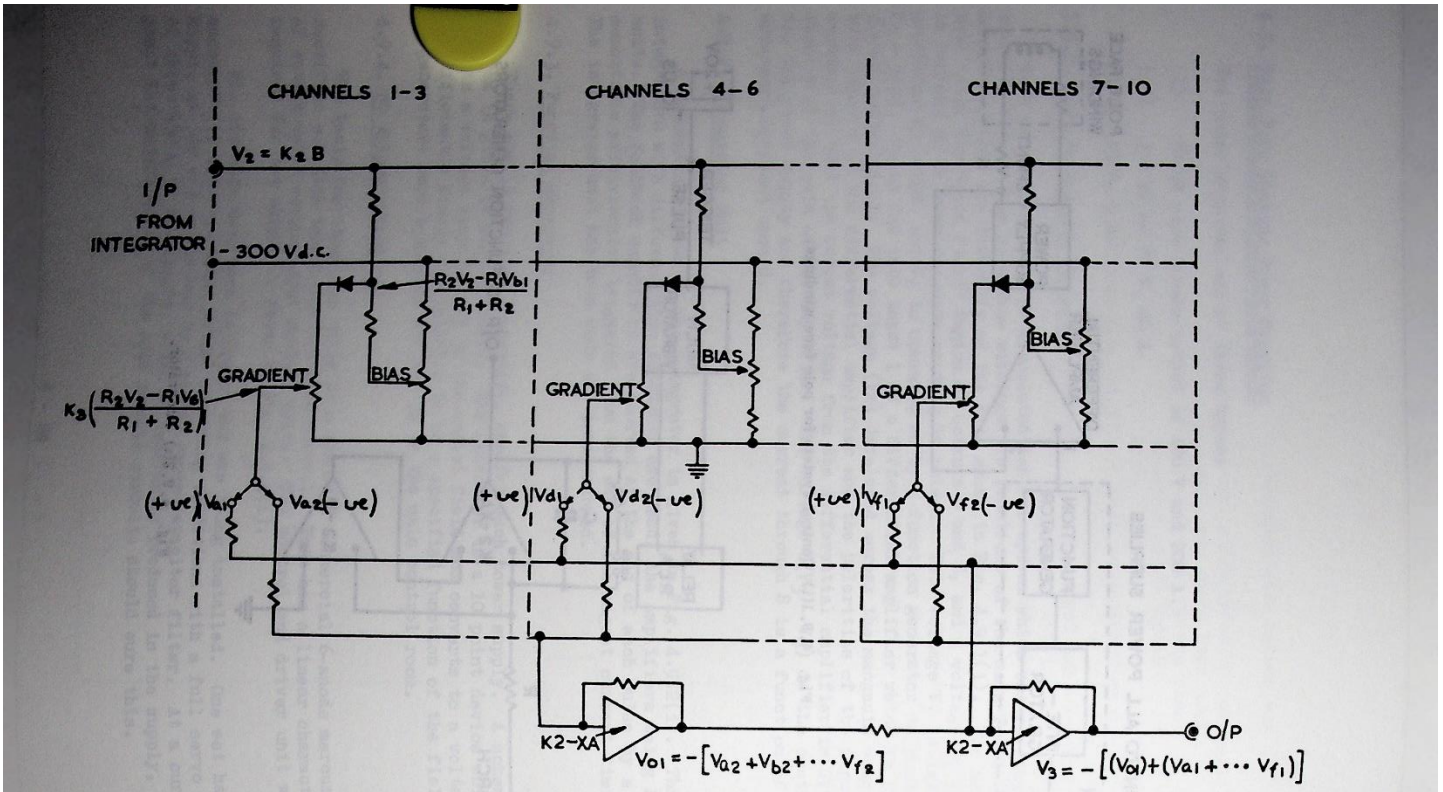

Fig. 4.9.3(i) Function generator.

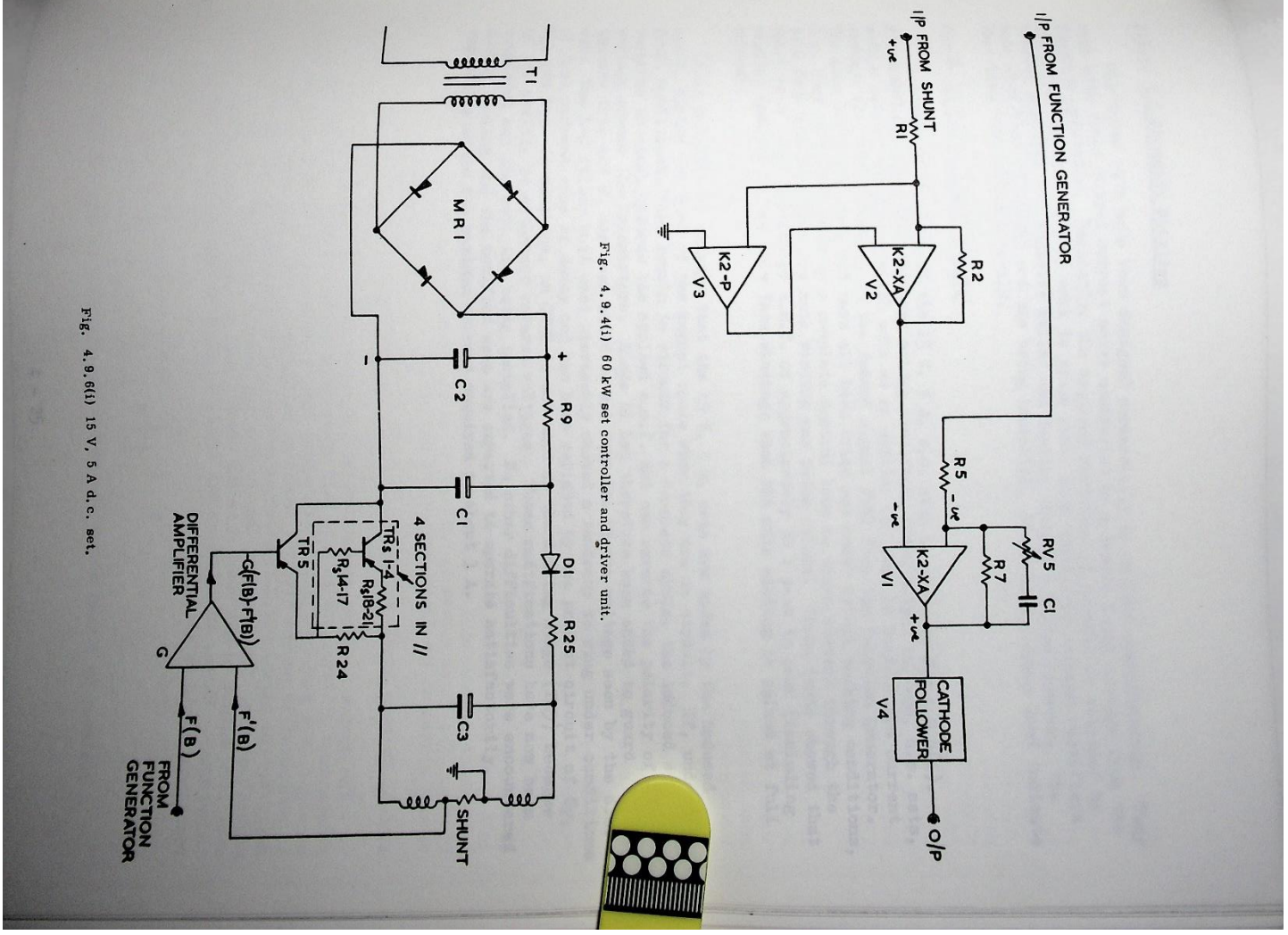

Fig. 4.9.4(i) 60 kW set controller and driver unit.

Fig. 4.9.6(i) 15 V, 5 A d.c. set.

4.9.5. 3.2 Kilowatt Supplies

The three sets have been designed commercially to outline specification. They each have their output current servo controlled by a demand input voltage from the function generator. Basically, the required variation of current is obtained by switching (using a varying mark to space ratio with controlled silicon rectifiers between positive and negative rails) and feeding through a filter network. The sets have been delivered and are being installed. Tests with a dummy load indicate that they work satisfactorily.

4.9.6. 15 Volt, 5 Amp Supply

A schematic diagram of the 15 V, 5 A, d.c. sets is given in Fig.4.9.6(i). Fundamentally these are ordinary bridge rectified, fixed output voltage, d.c. sets, with a series transistor which acts as an emitter follower to control the current through the load according to the demand signal F(B) from the function generator. The sets have been made and have all been tried out under actual working conditions, i.e. they have been used in a complete control loop to drive current through the pole face windings when the main winding was being pulsed. These tests showed that there is a large unbalanced e.m.f. of approximately 30 V peak to peak (including ripple) induced in the pole face windings when the main winding is pulsed at full current.

It is possible to arrange that the 15 V, 5 A, sets are aided by the induced e.m.f. during the part of the magnet cycle when they are in circuit. If, under fault conditions, they remain in circuit for a complete cycle, the induced e.m.f. reverses in sign, opposes the applied e.m.f. and can reverse the polarity of the voltage across the transistors. Diode D1 has therefore been added to guard against this and C_3 has been added to cut down the ripple voltage seen by the d.c. set. The L-C filter unit used previously showed a tendency to ring under conditions of fast current rise or decay and has been replaced by the present circuit of C_2, R_a, and C_1. In addition, an OC28 is now used as the driving stage (TR5) because of its ability to withstand reverse voltages. These modifications have now been completed and the sets are being installed. No other difficulties were encountered during testing and the modified sets are expected to operate satisfactorily, especially since the maximum current required is about 3 A.

4.10. Ripple Filter System

The power supply for the Nimrod magnet consists of two 24-phase grid controlled rectifier sets fed, via multi-phase transformers, from two tandem coupled motor-alternator-flywheel sets (see Section 5 of this report). The rectifier output has an inherent ripple voltage of approximately saw-tooth shape, of (nominally) 1200 c/s (the actual frequency varies over the period of a magnet pulse from 1123 c/s to 1164 c/s, dependant on the slip frequency of the slip-ring driving motors). The amplitude of this ripple varies during the course of a pulse. During flat-top it was found to have a maximum value of approximately 1200 V peak to peak (for each half of the power plant). This was observed during commissioning tests on the power plant and may ultimately be reduced. It was also observed that, during current decay, the ripple voltage rose to about 3000 V peak to peak. Additionally, the rectifier output contained a 100 c/s (nominal) component of about 175 V peak to peak amplitude. (This has since been reduced).

The effect of these ripple voltages on the operation of the proton synchrotron is particularly significant during flat-top[14]. Under this condition the ripple will modulate the spiral rate of the proton orbits, the degree of modulation being indicated by the ratio of E to V-IR, where E is the peak ripple voltage, V the mean voltage applied to the magnet during the flat top period, and IR is the ohmic drop in the magnet coil. For a flat-top duration of 0.5 s, V-IR has a value of about 50 V for the whole magnet, hence the ripple voltages referred to above will give a degree of modulation considerably greater than 100%; consequently, unless some form of ripple filter is employed, it will be impossible to spiral the beam smoothly onto a target. It is estimated that it will be necessary to reduce the ripple flux by a factor of 100 for satisfactory operation with a 0.5 s flat-top.

There are two ways of reducing the ripple flux in the magnet gap. The first method is to reduce the ripple voltage at the magnet terminals by developing a voltage, in phase opposition to that from the rectifiers, across an inductor placed in series with the rectifiers and magnets. The second method is to place an auxilliary winding around the magnet pole-pieces and use this to produce a flux acting so as to reduce the ripple flux in the useful region of the magnet gap. Both these systems will be employed on Nimrod to give the required reduction of ripple. The first system is referred to as the "primary ripple filter", the second system as the "secondary ripple filter".

4.10.1. Primary Ripple Filter

The system is shown schematically in Fig.4.10.1(i). It consists of two independant filters, one in each half of the magnet power supply. Each filter consists of a push-pull amplifier feeding into a transformer, the secondary of which is connected in series with the rectifier and magnet coils. The input to the amplifier is taken, via d.c. blocking capacitors, from across the ends of the magnet octants. The input voltage is thus the residual ripple E^1 and the amplifier output is GE^1 where G is the overall gain of amplifier and output transformer. Hence, if E denotes the ripple produced by the rectifiers, the resultant ripple is given by:-

$$E^1 = \frac{E}{1 + G}$$

A resistor is placed across the transformer secondary to damp out any

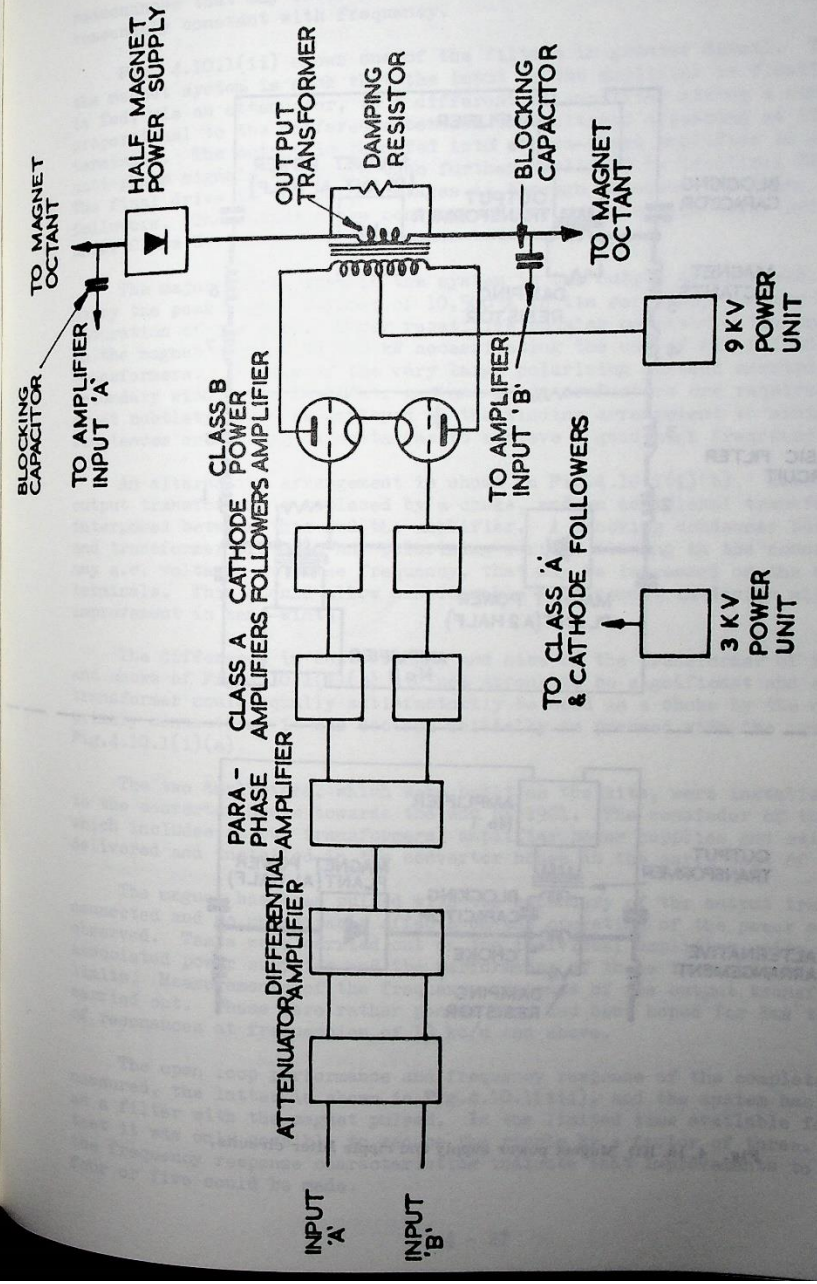

Fig. 4.10.1(ii) Schematic diagram of ripple filter amplifier.

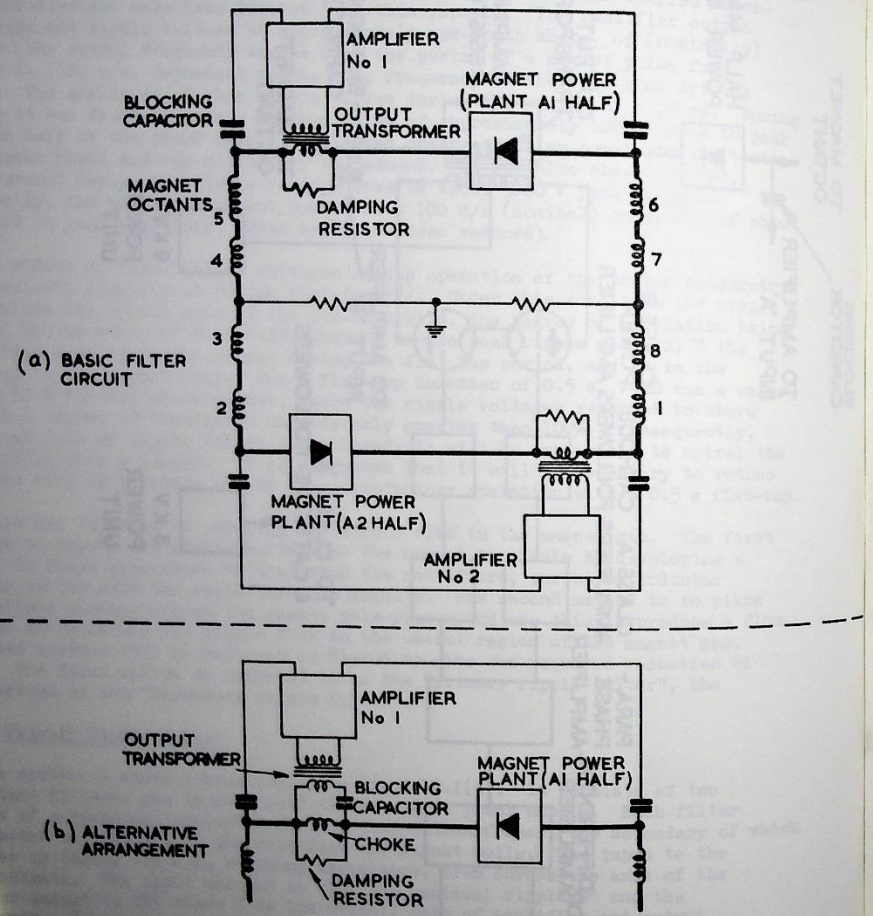

Fig. 4.10.1(i) Magnet power supply and ripple filter circuits.

reasonances that may occur and to present the amplifier with a load that is reasonably constant with frequency.

Fig. 4.10.1(ii) shows one of the filters in greater detail. The earthing of the magnet system is such that the input to the amplifier is floating. The input is fed, via an attenuator, to a differential amplifier giving a single output proportional to the difference between the voltages appearing at its two input terminals. The output is then fed into a para-phase amplifier to give two equal anti-phase signals which are then further amplified by identical Class A amplifiers. The final drive to the output stages is through impedance matching cathode followers. The output stage consists of two water cooled power triodes operating under Class B push-pull conditions.

The major single item in the system is the output transformer. This has to carry the peak magnet current of 10,500 A in its secondary winding without saturation of the core. Under repetitive pulsing conditions the copper loss due to the magnet current is 100 kW necessitating the use of oil filled water cooled transformers. In view of the very large polarising current carried by the secondary winding, a large air gap and heavy conductors are required and no very great subtlety could be employed in the winding arrangement to minimise leakage reactances or winding capacitances to achieve a good high frequency response.

An alternative arrangement is shown in Fig.4.10.1(i)(b). Here the original output transformer is replaced by a choke, and an additional transformer is interposed between this and the amplifier. A blocking condenser between the choke and transformer prevents any polarising current flowing in the secondary and limits any a.c. voltages at pulse frequency, that may be impressed on the secondary terminals. This should allow considerable improvement in design with consequent improvement in band-width.

The difference in cost, weight and size of the transformer of Fig.4.10.1(i)(a) and choke of Fig.4.10.1(i)(b) did not appear to be significant and since the transformer could equally satisfactorily be used as a choke by the omission of the primary connections it was decided initially to proceed with the arrangement of Fig.4.10.1(i)(a).

The two amplifiers, which were built on the site, were installed in the annexe to the convertor house towards the end of 1961. The remainder of the equipment, which includes output transformers, amplifier power supplies and switchgear, was delivered and installed in the convertor house in the early part of 1962.

The magnet has been pulsed with the secondary of the output transformers connected and no undesirable effects on the operation of the power supply were observed. Tests were carried out on the individual amplifier units and their associated power supplies and the performance of these is within the required limits. Measurements of the frequency response of the output transformers were also carried out. These were rather poorer than had been hoped for due to the occurrence of resonances at frequencies of 10 kc/s and above.

The open loop performance and frequency response of the complete system was measured, the latter is shown in Fig.4.10.1(iii), and the system has been operated as a filter with the magnet pulsed. In the limited time available for this latter test it was only possible to reduce the ripple by a factor of three. A study of the frequency response characteristics indicate that improvements to a factor of four or five could be made.

An alternative system in which a fraction of the ripple voltage appearing across the rectifier is fed into the amplifier was also tried. This does not comprise a feed-back loop and hence no problem of stability arises. However, in this system, the amplifier gain and phase shift is very critical and the results were not very much better than with the original system. Again careful design of phase correcting networks would improve this; however it would not appear to be possible to compensate for the slight changes in gain and phase of the output transformer which occur during pulsing, owing to the change in polarising current in the secondary winding. Consequently it would not seem likely that a reduction factor of better than five could be obtained.

In order to achieve the required factor of ten or better it will be necessary to change to the arrangement shown in Fig.4.10.1(i)(b). A specification for a suitable transformer has been drawn up and enquiries regarding its manufacture are in hand.

A further problem arises due to the fact that the 100 c/s ripple component is greater than had been hoped for. The original scheme did not provide for any filtering of components below 1200 c/s although a sufficient margin was allowed in the rating of the amplifier for these to be handled. A difficulty arises here since, if the bandwidth of the system is extended down to 100 c/s, then it will also attempt to respond to the changes in magnet voltage which occur during pulsing. This would result in saturation of the amplifier. However, the 100 c/s component is sufficiently small to be neglected except during flat-top and it should be possible to overcome the difficulty by a switching arrangement whereby the low frequency cut-off is only extended during the flat-top period.

4.10.2. Secondary Ripple Filter

The secondary ripple filter is designed to reduce the ripple field in the magnet gap by a factor of 20. The principle of the ripple correction network to be used is shown in Fig.4.10.2(i). The search coil samples the field in the good field region of the magnet gap. An amplifier drives a current through the correction windings in such a way as to oppose the field producing the search coil voltage.

Suppose search coil and correction coil have a mutual inductance M. Then a current I in the correction coil will produce a voltage $V = j\omega MI$ in the search coil, thus the output voltage is shifted through 90° and increases with frequency. The resulting 6 dB/octave slope of the open loop response may be corrected by the introduction of a circuit with a sinusoidal response of the form $e_{out} \alpha \frac{1}{j\omega} e_{in}$.

This may conveniently be done with an integrating circuit. The whole circuit is considered below.

(a) Design of the Ripple Chain

Suppose the unit consists of an integrator with time constant CR, an amplifier of gain G and a current amplifier of sensitivity S A/V. (see Fig.4.10.2(ii)).

To reduce ripple by a factor of 20:-

$$\frac{Vout}{Vin} = 19$$

But $$\frac{Vout}{Vin} = \frac{MGS}{CR}$$

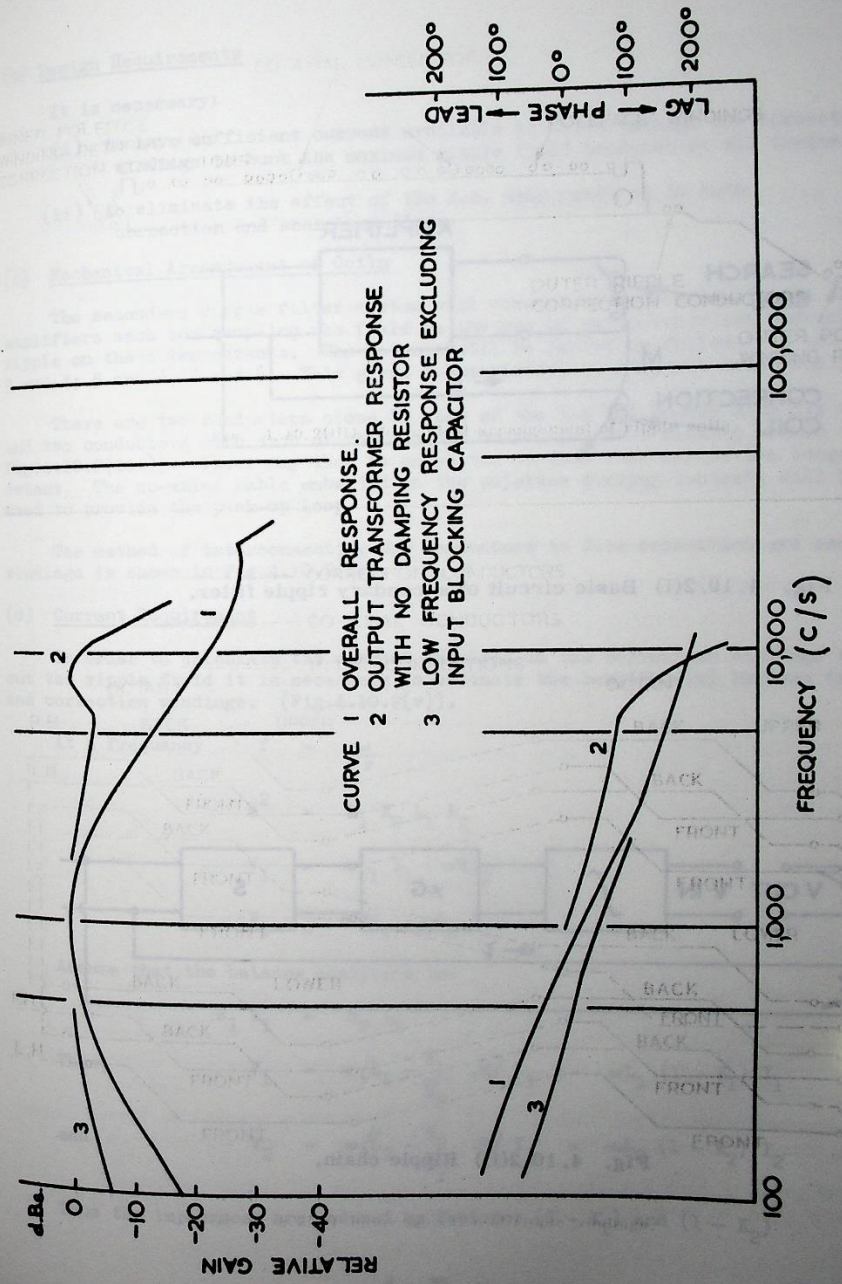

Fig. 4.10.1(iii) Ripple filter frequency response.

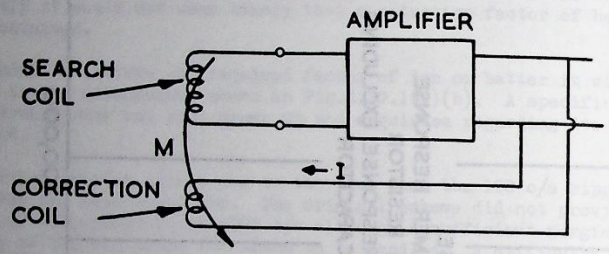

Fig. 4.10.2(i) Basic circuit of secondary ripple filter.

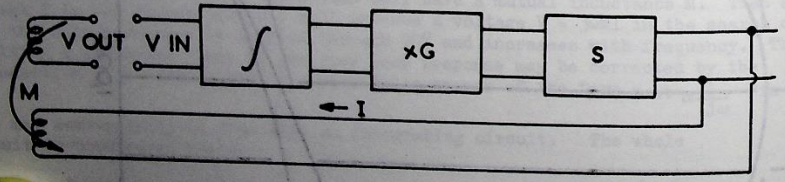

Fig. 4.10.2(ii) Ripple chain.

(b) Design Requirements

It is necessary:

(i) to have sufficient current available to drive through the correction windings to buck the maximum ripple field produced at all frequencies.

(ii) to eliminate the effect of the d.c. step produced in both correction and search windings.

(c) Mechanical Arrangement of Coils

The secondary ripple filter system will consist of four separate and independent amplifiers each one sampling the field in the gap of two octants and correcting the ripple on these two octants. The octants will be paired as follows: 1 and 2; 3 and 4; 5 and 6; 7 and 8. This gives a symmetrical arrangement azimuthally.

There are two conductors close to each of the top and bottom main lip coils, and two conductors with each of the top and bottom poleface winding return (see Fig.4.10.2(iii)). These may then be connected to form four correction loops per octant. The co-axial cable embedded in the poleface winding laminate will be used to provide the pick-up loop.

The method of interconnecting the conductors to form correction and search windings is shown in Fig.4.10.2(iv).

(d) Current Requirement

In order to calculate the current required in the correction windings to buck out the ripple field it is necessary to estimate the coupling (k) between the main and correction windings. (Fig.4.10.2(v)).

At a frequency $f = \frac{\omega}{2\pi}$

$$M^2 = K_1 K_2 L_1 L_2$$

$$V_1 = \omega L_1 I_1 - \omega M I_2$$

$$V_2 = \omega M I_1 - \omega L_2 I_2$$

Assume that the balance condition is:

$$N_1 I_1 = N_2 I_2$$

Then, $$V_1 = \omega \left[L_1 - \frac{N_1}{N_2} . M \right] I_1 = \omega L_1 (1 - K_1) I_1$$

and $$V_2 = \omega \left[L_2 - \frac{N_2}{N_1} . M \right] I_2 = -\omega L_2 (1 - K_2) I_2$$

Thus the impedances are reduced by factors: $(1 - K_1)$ and $(1 - K_2)$

When the secondary is open circuit,

$$V_1 = \omega L_1 I_1$$

$$V_2 = \omega M I_1$$

From this L_1 and M can be deduced. L_2 can be found similarly by considering the primary open circuit. K_1 and K_2 can then be deduced.

Since the Nimrod magnet was not available, coils were wound on magnet Model V to simulate correction windings, and values of L_1 and L_2 and M (and hence K_1 and K_2) were obtained by experiment, at frequencies from 25 c/s to 120 kc/s. From these results and the physical parameters of Nimrod it is possible to estimate the current required to buck the expected ripple field.

These parameters are shown in Table 4.10.2(I).

TABLE 4.10.2(I)

Number of:-	Nimrod (one octant)	Magnet Model V
Polepieces (main coil)	42	8 (effectively)
Polepieces (correction coil)	42	4
Main coil turns	42	160
Correction coil turns	4	20

Considering inductance as being proportional to area and $(\text{turns})^2$ it follows that:-

$$L_p = 0.724\, L_M$$

$$L_B = 0.84\, L_C$$

where L_p is the inductance of Nimrod main coil (over 2 octants)

L_B is the inductance of Nimrod correction coil (over 2 octants)

L_M is the inductance of Model V main coil

L_C is the inductance of Model V correction coil

The ripple potential for each half of the power supply applied to Nimrod magnet before any form of ripple correction may be 600 V peak to peak (at 1135 c/s).

If the primary ripple filter reduces this to $^1/_{10}$ the ripple potential becomes 60 V peak to peak across 2 quadrants or 30 V peak to peak across 2 octants.

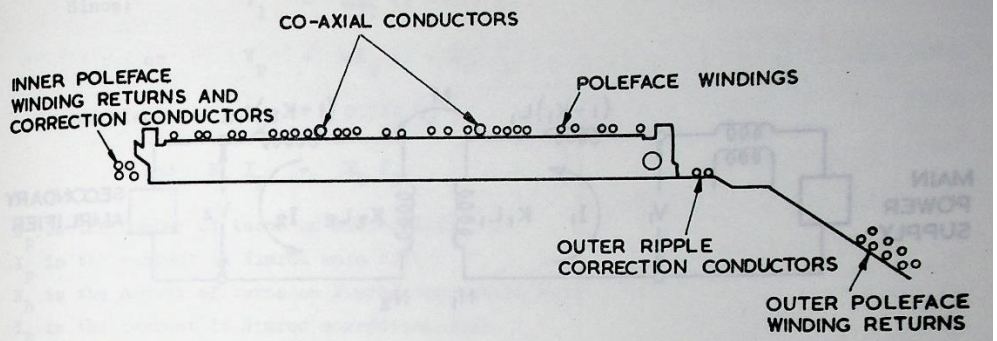

Fig. 4.10.2(iii) Mechanical arrangement of ripple coils.

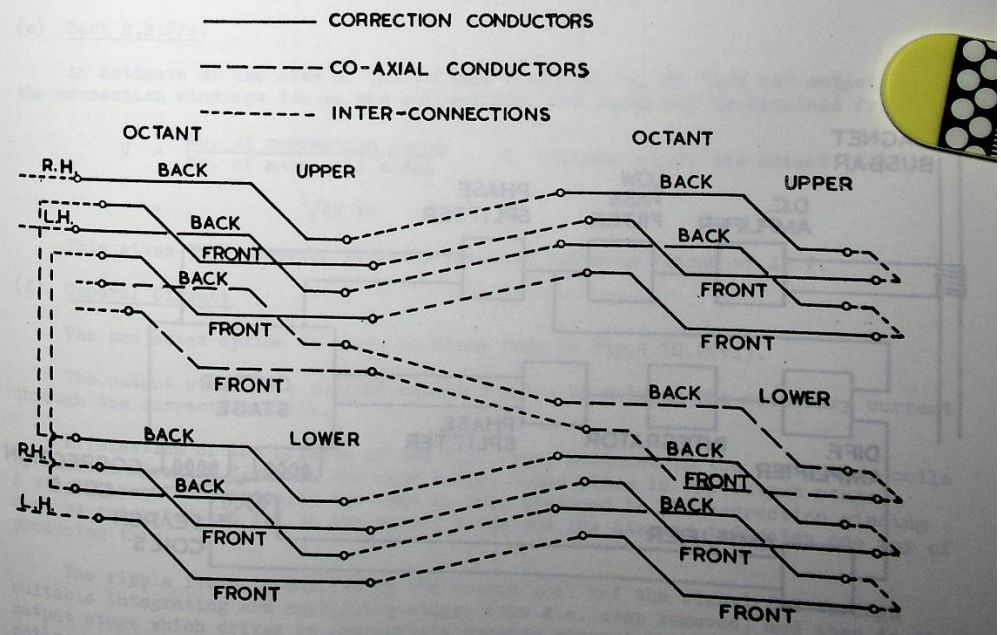

Fig. 4.10.2(iv) Interconnection of ripple windings.

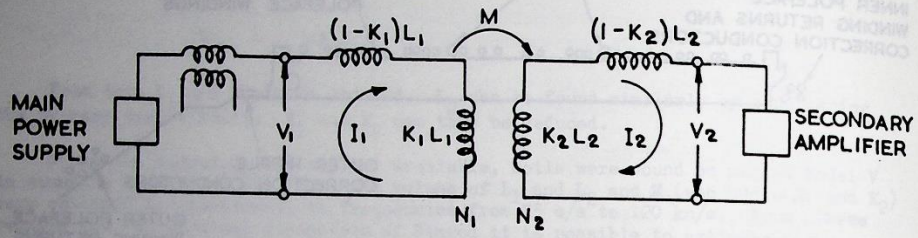

Fig. 4.10.2(v) Basic circuit for secondary ripple filter.

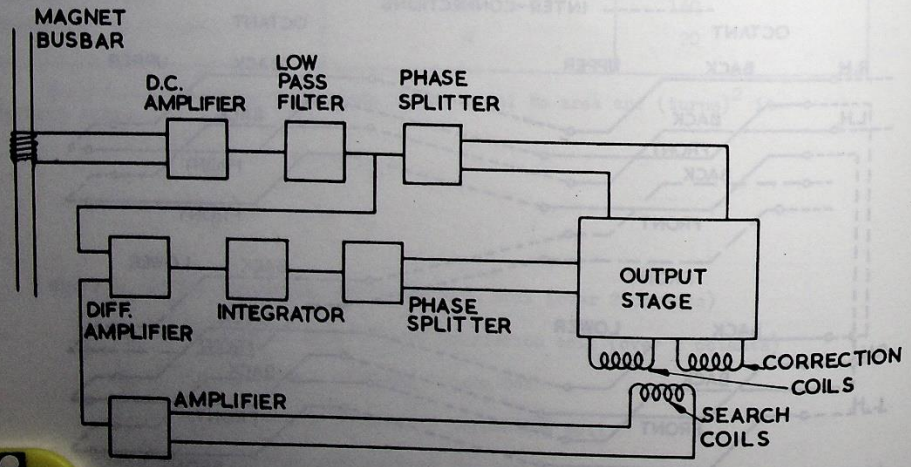

Fig. 4.10.2(vi) General circuit for secondary ripple filter.

Since: $V_1 = \omega L_1 (1 - K_1) I_1$

or $V_p = \omega L_p (1 - K_1) I_p$

and also: $L_p = 0.724 L_M$

and $N_p I_p = N_B I_B$

N_p is the number of turns on Nimrod main coil
I_p is the current in Nimrod main coil
N_B is the number of turns on Nimrod correction coil
I_B is the current in Nimrod correction coil

Hence: I_B =450 mA is obtained at 1135 c/s

Also since $V_B = \omega L_B (1 - K_2) I_B$

V_B = 2 volts is obtained at 1135 c/s

(e) Back E.M.F's.

An estimate of the size of the voltage V induced in one turn per octant of the correction windings due to the current rise and decay may be obtained from:

$$V = \frac{\text{No. of correction turns}}{\text{No. of main coil turns}} \times \text{Voltage across one octant (Vo)}$$

$$= \frac{1}{42} Vo$$

This gives 50 V compared with the measured value on Nimrod of 42 V.

(f) General Circuit

The projected system is shown in block form in Fig.4.10.2(vi).

The output stage is a current source capable of driving the necessary current through the correction coils.

Elimination of the effects of the d.c. step, produced in the correction coils by current rise and decay in the main coils, takes place in the output stage. A step voltage substantially the same as that produced in the correction winding must be generated and fed to the output stage and the diagram indicates one way of producing this.

The ripple field is sampled by the search coil and the signal fed through suitable integrating and amplifying stages (the d.c. step removed) and then to the output stage which drives an appropriate bucking current through the correction coils.

(g) Tests on Magnet Model V

Prototypes of the output stage and the servo system have been constructed and measurements carried out on magnet Model V to check the values of current required to buck the ripple field. The ripple field was produced by using an external amplifier. The system operated on a closed servo loop and reduction factors of 17 were obtained for various frequencies of ripple at amplitudes within the designed range.

(h) Tests on the Nimrod Magnet

Using the primary ripple filter as an external source, ripple was fed to the Nimrod magnet and measurements were made to check the calculations of the bucking currents required at various frequencies. At 1000 c/s, 0.420 A were required to buck 30 V of ripple compared with a computed value of 0.5 A. The discrepancy is probably due to the differences between Model V and the Nimrod magnet resulting from the very different lengths, and variation in positions of the coils.

The frequency response of the output stage was investigated using the Nimrod correction coils and the search coils. Further investigations will be required.

(i) Frequencies below 1200 c/s.

Detailed measurements of the ripple on the Nimrod power supplies have shown that considerable ripple is present at frequencies very much lower than those anticipated. Since the current required for bucking is approximately inversely proportional to frequency, it will probably be necessary to redesign the output stage to cope with the extra current requirements.

4.11. Peaking Strips

The peaking strip and associated equipment determines the starting point for the primary frequency generator by giving out a trigger pulse when the field in the magnet gap passes through a pre-set value: it is needed because the starting point of the field in the magnet is variable due to the remanent field.

The principle of the device depends on the fact that only a small field change is required to alter the flux in mu-metal from saturation in one direction to saturation in the other direction. Since this reversal occurs at around zero field, it can be used as a null detector indicating when the magnet field becomes equal to a reference field applied to it in the opposite direction.

The layout is shown in Fig. 4.11(i). The bias solenoid produces a field along its axis in the opposite direction to the magnet field in which it is placed. A small piece of mu-metal wire is supported at the centre and when the rising magnet field equals the solenoid field a flux change occurs in the wire which generates a pulse in the pick-up coil wound on it. The signal to start the primary frequency generator is derived from this pulse.

The bias solenoid has 20,000 turns of 30 s.w.g. enamelled copper wire producing a field of 120 gauss with about 47 mA. The mu-metal wire is $2\frac{1}{2}$ in long by 4 thou. in diameter and the pick-up coil has 3,000 turns of 50 s.w.g. enamelled copper wire. In a field changing at the rate of 10 kG/s the pulse shown in Fig.4.11(ii) is produced.

An overall long term stability in field of 1 part in 10,000 was required. The system is made up of a number of components each of which contributes to the total variation and it is necessary to attempt to reduce each contribution to 1 part in 100,000. The two main parts are the bias current source and the pulse circuitry.

4.11.1. Bias Current Source

Fig.4.11.1(i) shows the basic circuit used to provide a stable current for the bias solenoid. Factors causing variation were:

(a) Series Resistor R

This was made of manganin which has a temperature coefficient of about 1 part in 100,000 per °C. The ambient temperature variation catered for was 18-32°C and it was mounted in an aluminium block thermostatically controlled to 1°C with a contact thermometer.

(b) Reference Potential, e_R

The circuit is shown in Fig.4.11.1(ii). Leading from a stabilised -300V line, two extra stages of stabilisation are provided by zener diodes. The final pair (X_3 and X4) have a temperature coefficient of less than 1 part in 100,000 per °C and are also mounted in the thermostatically controlled block.

(c) Noise and Hum

The reference potential is about 10 V so that any noise generated in the

summing resistors should be kept down to 100 μV. Any current flowing through the bias solenoid but not through R, or through R but not through the bias solenoid as a result of stray capacitance causes error. At the minimum bias current of the range (30 mA) the noise current needs to be not more than 0.3 μA a.c. peak to peak. Mains wiring can feed about 2 μA a.c. to earth into any unscreened conductors via the stray capacitance so that screening of every part of the solenoid circuit is necessary.

(d) Voltages Induced by the Magnet Field

A voltage proportional to the magnet supply voltage is induced in the bias solenoid. This has a d.c. and an a.c. component, the latter having a fundamental component of about 1200 c/s. At these frequencies the capacitance of the cable connecting the solenoid to the stabiliser and the capacitance of the solenoid itself, bypass the stabiliser. The solenoid is in fact self-resonant at around 8 kc/s but fortunately at 1 kc/s it is sufficiently off the resonance. The effect of the cable capacitance is reduced by backing off the voltage in the solenoid with an identical one placed next to it connected in series opposition.

4.11.2. Pulse Circuitry

A change of 0.6 gauss is needed to drive the mu-metal from saturation to saturation so it is not accurate enough just to use the output pulse without further treatment. Amplitude selection off one edge of the pulse was rejected because the height is proportional to rate of change of magnet field. The pulse is integrated to give an output proportional to flux density in the mu-metal which is directly related to the magnet field. A stable trigger circuit is operated when it reaches a pre-set level.

4.11.3. Mechanical Construction

The magnetic properties of mu-metal are destroyed by any permanent physical deformation and the wire is very thin so the pick-up coil is wound on a thin walled glass capillary tube (o.d. 23 thou.) and the wire threaded down afterwards. The coil is insulated and screened with 1 thou. copper foil and 1 thou. Micalex. The connections are then brought out in a tail of 34 s.w.g. enamelled copper wire and the final o.d. is approximately 130 thou. For protection this rather delicate assembly is cast in a cold setting Araldite to an o.d. of 0.145 in.

The bias solenoid design is limited by power dissipation since heat can be removed only by radiation. For a multi-layer solenoid the dissipation is determined by its dimensions, the field and the specific resistance of copper and is reduced by making the ratio of inner radius to outer radius as small as possible. This has led to using the solenoid without any former at all. The wire is wound onto a former which is removed after the wire has been set in Araldite. The dimensions are shown in Fig.4.11(i). The power is reduced further by placing the peaking strip assembly in the fringe field of the magnet where it operates at half the gap field.

The assembly is situated in the high vacuum region and consequently is covered with metal to reduce outgassing. This is done by electroplating with copper. Unfortunately a continuous metal surface like this constitutes an unpleasant shorted turn which would modify the field locally in an unpredictable way so it is necessary to break up the surface. All the metal has to be earthed to stop it charging up. Both these objects are achieved by etching vertical lines, using

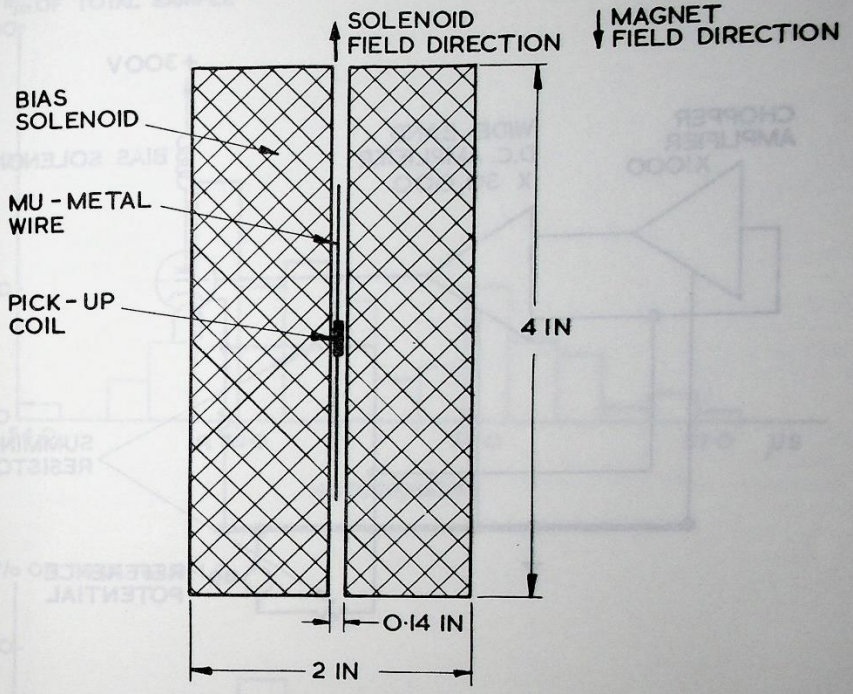

Fig. 4.11(i) Layout of peaking strip.

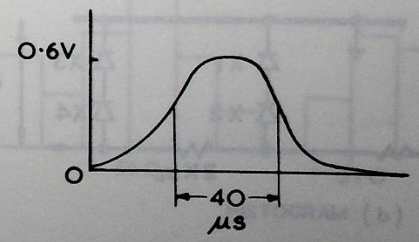

Fig. 4.11(ii) Pulse from peaking strip.

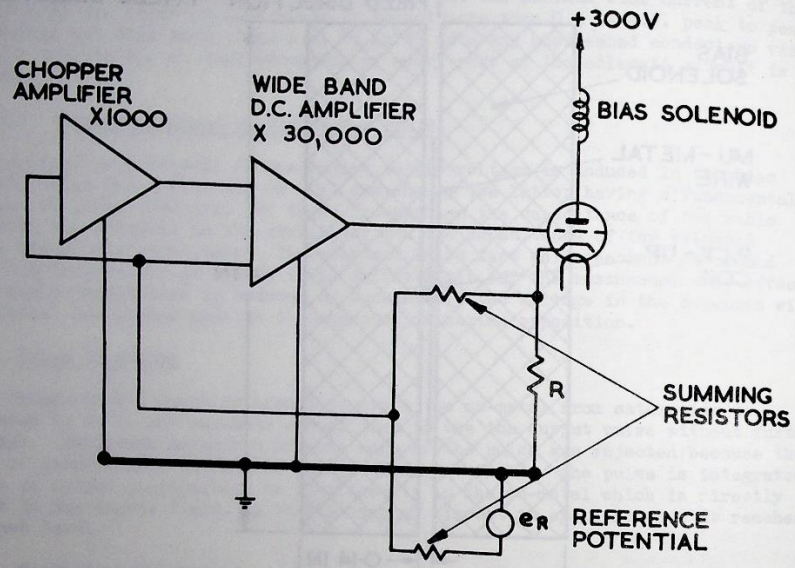

Fig. 4.11.1(i) Basic circuit of current stabiliser for peaking strip.

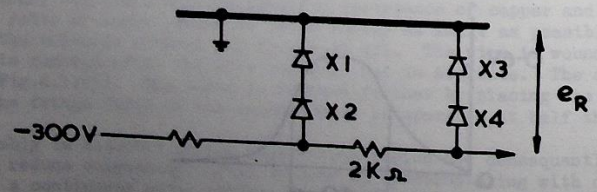

Fig. 4.11.1(ii) Reference potential supply.

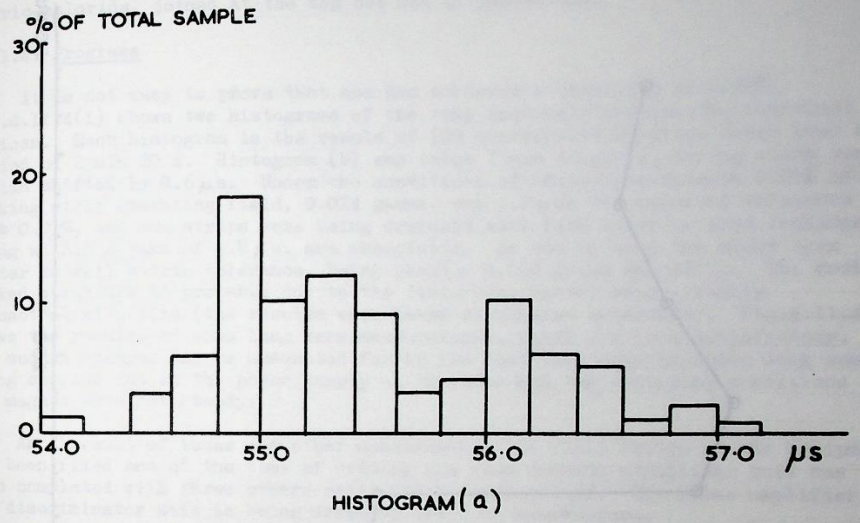

HISTOGRAM (a)

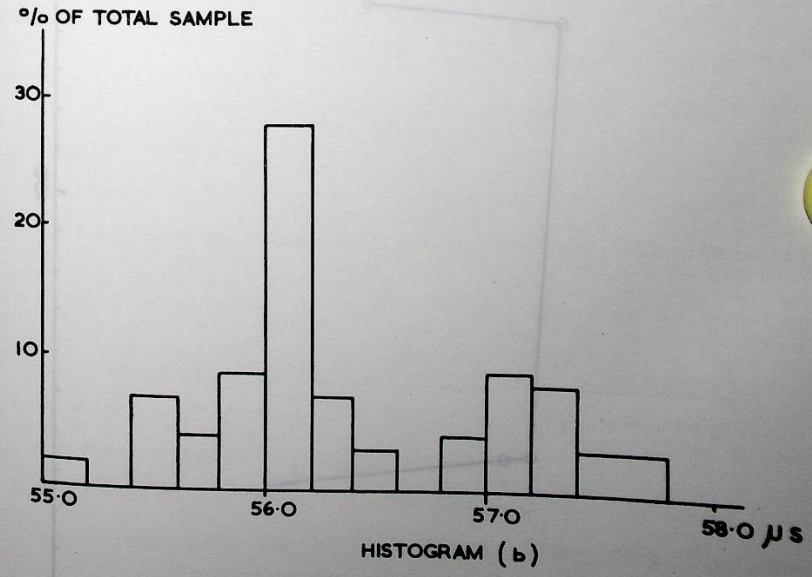

HISTOGRAM (b)

Fig. 4.11.4(i) Time between two peaking strip pulses.

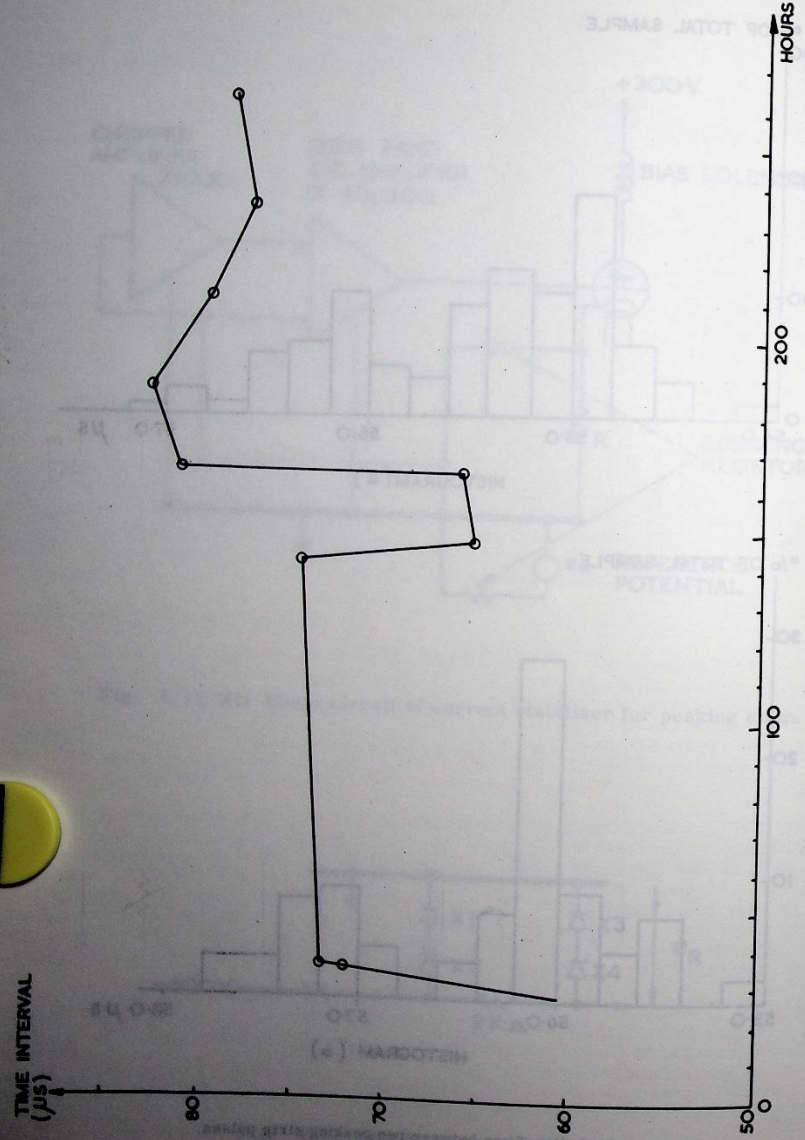

Fig. 4.11.4(ii) Long term drift of peaking strip.

ferric-chloride, joined at the top but not at the bottom.

4.11.4. Progress

It is not easy to prove that one has achieved a stability of 0.01%. Fig.4.11.4(i) shows two histograms of the time intervals between two identical devices. Each histogram is the result of 100 consecutive readings taken over a period of 2 min 20 s. Histogram (b) was taken 7 min after (a) during which the median shifted by 0.6 μs. Under the conditions of these measurements 0.01% of the peaking strip operating field, 0.024 gauss, was 1.2 μs; the required tolerance is ± 0.01%, and two strips were being compared with each other so that readings lying within a band of 4.8 μs. are acceptable. As can be seen the short term jitter is well within tolerance, being about ± 0.010 gauss per strip. The double peaked structure is probably due to the disturbing factor being roughly sinusoidal with time (the results were taken at regular intervals). Fig.4.11.4(ii) shows the results of some long term measurements, which are less satisfactory. The sudden changes may be accounted for by the fact that commissioning work was being carried out on the power supply at the time and the operating conditions of the magnet were not steady.

As a result of these and other measurements the final design of the equipment has been fixed and at the time of writing one bias current stabiliser unit has been completed with three others still under construction. The pulse amplifier and discriminator unit is being drawn up prior to manufacture.

REFERENCES FOR SECTION 4.

1. J.J. Wilkins and A.J. Egginton. A.E.R.E. GP/R 2181. 1957.
2. P. Bowles. Nuclear Engineering. April 1959.
3. G.W. Dixon and A.G. Entwistle. Nuclear Engineering. April 1959.
4. D.A. Gray et al. NIRL/R/4, 1963.
5. A.J. Holt and J.D. Milne. A.E.R.E. R 3312, 1960.
6. J.J. Wilkins and D.A. Gray. NIRL/R/33, 1963.
7. D.A. Gray, A.H. Spurway and J.J. Wilkins. A.E.R.E. A/R 2626.
8. D.A. Gray, A.H. Spurway and J.J. Wilkins. A.E.R.E. A/R 2845.
9. G. Bronca et al. L'onde Electrique No.387. 463, June 1959.
10. J.J. Wilkins and A.H. Spurway. NIRL/R/6, 1962.
11. A.J. Holt and J.D. Milne. NIRL/R/3, 1961.
12. J.P. Blewett et al. R.S.I. 24, 773, Sept. 1953.
13. P.F. Smith. A.E.R.E. A/R 2849, 1959.
14. J.J. Wilkins. A.E.R.E. R. 1860, 1959.

SECTION 5

MAGNET POWER SUPPLY

5.1. Introduction

The Nimrod magnet power supply plant comprises two 60 MW motor-alternator-flywheel sets which power the magnet via a mercury arc convertor installation of similar rating supplied from the alternators through phase splitting transformers giving 24 phase operation.

This report covers the period up to 31st December, 1962 and does not refer to details of design. These design aspects, with indications of the historical reasons for adopting the final design chosen are given in the following three papers published in Proc. I.E.E., Vol. 110, No. 3, March 1963.

Paper 1 General
Paper 2 Rotating machines
Paper 3 Mercury arc convertors

All three papers have the main title:- 'Magnet Power Supply for the 7 GeV Proton Synchrotron Nimrod'.

The main power circuit is shown in Fig. 5.1(i).

The first 60 MVA motor-alternator-flywheel set was commissioned for open circuit running conditions during the last two months of 1961 and it was then used to carry out preliminary 'on load' commissioning using each half of the convertor installation in turn, with four of the magnet octants as load, during the first quarter of 1962. From April 1962 until the end of August 1962 one motor-alternator-flywheel set and one half of the convertor plant was used to pulse the magnet (four octants at any one time) in order that the magnetic survey could be carried out.

The second alternator was delivered at the beginning of September 1962. Installation was completed in about six weeks and the second motor alternator flywheel set ran up to speed for the first time on 21st October, 1962.

After further commissioning, and also re-alignment of the first motor-alternator-flywheel set to the recently installed second set, the final fitted bolts and bushes were installed in the flywheel to flywheel coupling and on 21st November, 1962 the complete rotary plant on its common 100 ft long solidly connected shaft system ran up to speed for the first time. On load testing and final commissioning could not be carried out immediately since the magnet was not available. Detailed final commissioning of power supplies was planned for January 1963 using four magnet octants and February 1963 using the whole of the magnet. This period will be covered in the second part of this report.

However, early experience on the plant has shown that when the plant is operating at its full thermal rating, pulse repetition rates will be at least 10% higher than those quoted in the design stages.

The following general operational information may be of interest:

Total running hours from October 1961-31st December, 1962 ..	1,600
Total pulsing hours	700
Pulsing hours at standard pulse and/or standard pulse +15%	460